ACS Infectious Diseases

pubs.acs.org/journal/aidcbc

Article

Disparate Regions of the Human Chemokine CXCL10 Exhibit Broad-Spectrum Antimicrobial Activity against Biodefense and Antibiotic-Resistant Bacterial Pathogens

Matthew A. Crawford, Amanda E. Ward, Vincent Gray, Peter Bailer, Debra J. Fisher, Ewa Kubicka, Zixian Cui, Qinmo Luo, Mary C. Gray, Alison K. Criss, Lawrence G. Lum, Lukas K. Tamm, Rachel A. Letteri, and Molly A. Hughes*

Cite This: *ACS Infect. Dis.* 2023, 9, 122−139

Read Online

ACCESS | Metrics & More | Article Recommendations | Supporting Information

ABSTRACT: CXCL10 is a pro-inflammatory chemokine produced by the host in response to microbial infection. In addition to canonical, receptor-dependent actions affecting immune-cell migration and activation, CXCL10 has also been found to directly kill a broad range of pathogenic bacteria. Prior investigations suggest that the bactericidal effects of CXCL10 occur through two distinct pathways that compromise the cell envelope. These observations raise the intriguing notion that CXCL10 features a separable pair of antimicrobial domains. Herein, we affirm this possibility through peptide-based mapping and structure/function analyses, which demonstrate that discrete peptides derived from the N- and C-terminal regions of CXCL10 mediate bacterial killing. The N-terminal derivative, peptide P1, exhibited marked antimicrobial activity against *Bacillus anthracis* vegetative bacilli and spores, as well as antibiotic-resistant clinical isolates of *Klebsiella pneumoniae*, *Acinetobacter baumannii*, *Enterococcus faecium*, and *Staphylococcus aureus*, among others. At bactericidal concentrations, peptide P1 had a minimal degree of chemotactic activity, but did not cause red blood cell hemolysis or cytotoxic effects against primary human cells. The C-terminal derivative, peptide P9, exhibited antimicrobial effects, but only against Gram-negative bacteria in low-salt medium—conditions under which the peptide can adopt an α-helical conformation. The introduction of a hydrocarbon staple induced and stabilized α-helicity; accordingly, stapled peptide P9 displayed significantly improved bactericidal effects against both Gram-positive and Gram-negative bacteria in media containing physiologic levels of salt. Together, our findings identify and characterize the antimicrobial regions of CXCL10 and functionalize these novel determinants as discrete peptides with potential therapeutic utility against difficult-to-treat pathogens.

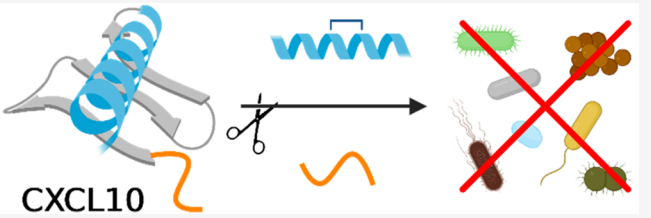

KEYWORDS: *chemokine, CXCL10, antimicrobial peptide, hydrocarbon staple, bacteria, antibiotic resistant*

Chemokines are a family of small signaling proteins best known for orchestrating the movement of immune cells during infection.[1] Chemokines elicit this and other host-targeted effects by activating corresponding G-protein-coupled receptors selectively expressed by responsive cells. In addition to receptor-dependent actions, a subset of chemokines also exerts direct antimicrobial effects against a wide array of bacterial, viral, protozoan, and/or fungal pathogens.[2−5] Chemokines have a highly conserved tertiary structure that consists of an unordered N-terminus, followed by an "N-loop", a three-strand antiparallel β-sheet, and a C-terminal α-helix that lies across the β-sheet.[6,7] This typified structure is stabilized by disulfide bonds formed between cysteine residues, the arrangement of which defines the major subfamilies of chemokines: CXC, CC, C, and CX3C (where C is cysteine and X is a non-conserved amino acid residue).[7] The predominant paradigm is that the N-terminal region drives cell-receptor binding/activation, while the C-terminal region mediates microbial killing.[8,9]

CXCL10, known originally as interferon γ-induced protein 10 kDa (IP-10), is a pro-inflammatory chemokine produced by a range of resident and immune cell types in response to infection and injury.[10] CXCL10 affects the movement and function of host cells that express the chemokine receptor CXCR3 (e.g., T cells, monocytes).[1] Besides host-targeted actions, a number of laboratories, including ours, have reported CXCL10 to kill both Gram-positive and Gram-negative bacterial pathogens *in vitro*, including *Bacillus anthracis* spores and bacilli, *Staphylococcus aureus*, and *Escherichia coli*, among others.[5,11−16] CXCL10 has also been found by our group to exert bactericidal effects against organisms identified as urgent

Received: September 4, 2022
Published: December 7, 2022

ACS Publications

© 2022 The Authors. Published by American Chemical Society

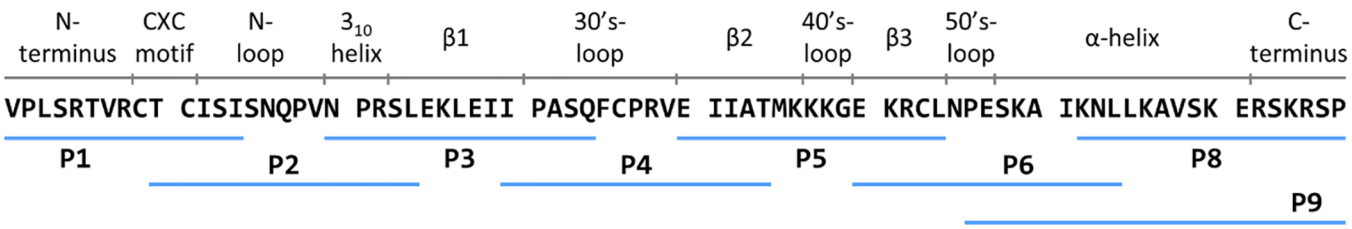

Figure 1. CXCL10-derived peptide library. The primary amino acid sequence of mature, secreted human CXCL10 (UniProtKB P02778) is shown in relation to major structural elements (Protein Data Bank 1O80/1LV9). Overlapping 14- to 22-mer peptides derived from CXCL10 and tested in this work are indicated: P1 (VPLSRTVRCTCISI), P2 (TCISISNQPVNPRSL), P3 (NPRSLEKLEIIPASQ), P4 (IPASQFCPRVEIIAT), P5 (EIIATMKKKGEKRCL), P6 (EKRCLNPESKAIKNL), P8 (KNLLKAVSKERSKRSP), and P9 (PESKAIKNLLKAVSKERSKRSP).

antibiotic-resistance threats by the U.S. Centers for Disease Control and Prevention (CDC), such as carbapenem-resistant *Enterobacteriaceae*,[17] as well as Gram-negative bacteria that are resistant to colistin, a last-line therapeutic for treating infections caused by multidrug-resistant (MDR) and extensively drug-resistant (XDR) bacteria.[18] That chemokine-mediated antimicrobial effects contribute to host defense against infection *in vivo* is evidenced by investigations using murine models of infection. For instance, we demonstrated that the neutralization of CXCL10 and/or CXCL9 (a closely related CXCR3 agonist that is also bactericidal[15,19]) increases host susceptibility to pulmonary infection by *B. anthracis*, independent of chemokine-receptor signaling.[14] This was similarly shown for enteric disease associated with *Citrobacter rodentium*.[20]

The capacity of CXCL10 to kill bacteria has been attributed to its C-terminal α-helix,[16] an amphipathic structure similar to that observed for many antimicrobial peptides, such as cathelicidins and magainins.[21] However, a C-terminally truncated CXCL10 protein that lacks this α-helical region retains much of its capacity to kill *B. anthracis*.[22] Moreover, previous genetic and biochemical studies conducted using *B. anthracis* indicate that the bactericidal effects of CXCL10 proceed via two distinct pathways: (i) dysregulation of peptidoglycan turnover through interaction with the surface-associated bacterial FtsE/X complex, which governs aspects of peptidoglycan incorporation and hydrolysis that are important to viability,[13,22,23] and (ii) a comparatively non-specific disruption of membrane barrier function that leads to permeabilization and bioenergetic collapse.[22,23] Given these prior findings, we hypothesized that CXCL10 features a separable pair of antimicrobial domains. Indeed, using peptide-based mapping and structure/function analyses, we show in the current study that disparate N- and C-terminal regions of human CXCL10 exert broad-spectrum antimicrobial effects against diverse biodefense and MDR/XDR pathogens. The identification and characterization of these novel bactericidal determinants provide unique insight into the pathogen-targeted actions of host chemokines and establish a practical foundation for the development of CXCL10-derived peptides to treat bacterial infections.

RESULTS

Antimicrobial Effects of CXCL10-Derived Peptides against *B. anthracis* Bacilli and Spores. Toward identifying the bactericidal region(s) of human CXCL10, we designed a series of overlapping 14- to 22-mer peptides derived from the full-length amino acid sequence of the mature chemokine (Figure 1). Bacterial killing by these individual peptides was tested against Gram-positive *B. anthracis* Sterne 7702 bacilli in Dulbecco's Modified Eagle Medium (DMEM) with 10% fetal bovine serum (FBS) using alamarBlue, a fluorescence-based viability reagent that generates results commensurate to those obtained by colony-forming unit (cfu) determination[15,24] and that has been used previously by our group, and others, to measure the antimicrobial effects of CXCL10.[12−15,22,25] Only peptide P1, derived from the unstructured N-terminus of CXCL10, was found to significantly reduce bacterial viability (Figure 2A); analogous killing was observed against the related organism *Bacillus subtilis* (Figure 2B). The bactericidal effects exerted by peptide P1 against *B. anthracis* vegetative bacilli were observed to be sequence specific (i.e., scrambling the native amino acid sequence abolished antimicrobial activity; Figure 2C) and concentration dependent, with a half-maximal effective concentration (EC_{50}) of 18.1 ± 0.3 μM (Figure 2D). Conspicuously, the concentration−response curve for peptide P1 against *B. anthracis* bacilli was non-linear and quite steep over the effectual range, possibly indicating positive cooperativity in oligomeric assembly and/or target binding.[26] Consistent with prior reports regarding full-length CXCL10,[13,22,23] *B. anthracis* bacilli lacking the FtsX component of the FtsE/X complex that regulates peptidoglycan hydrolase activity were less susceptible to killing by peptide P1 (EC_{50} of 53.1 ± 0.8 μM; Figure 2D).

To assess the potential of peptide P1 to exert antimicrobial effects against the dormant and hardy spore form of *B. anthracis*, light microscopy was used to visually monitor spore germination and the subsequent outgrowth of vegetative bacilli over time in Roswell Park Memorial Institute (RPMI) medium with 5% FBS (Figure 2E). Untreated spores, as well as those exposed to the non-antimicrobial CXCL10-derived peptide P5, were found to germinate and undergo extensive vegetative replication such that abundant chains of bacilli were observed after 6 h of incubation. Conversely, *B. anthracis* spores exposed to peptide P1 showed no morphologic signs of germination (e.g., swelling, elongation) and a complete absence of bacilli at 6 h. Expanded field-of-view images for each treatment group are provided in Figure S1. To quantify bacterial viability and discriminate between spore and bacilli forms of the organism, cfu determination was performed both before and after heat treatment (Figure 2F). Heat treatment kills germinating spores and vegetative bacilli, but not ungerminated spores. Thus, cfu counts prior to heating represent total viable organisms (all spores and bacilli), whereas counts obtained after heat treatment account only for dormant yet viable spores. Using the initial spore inoculum as a reference, heat-treated cfu counts obtained from untreated and peptide P5-treated sample groups decreased ~200-fold at 6 h (due to spore germination), and parallel counts without heat treatment increased more

https://doi.org/10.1021/acsinfecdis.2c00456
ACS Infect. Dis. 2023, 9, 122−139

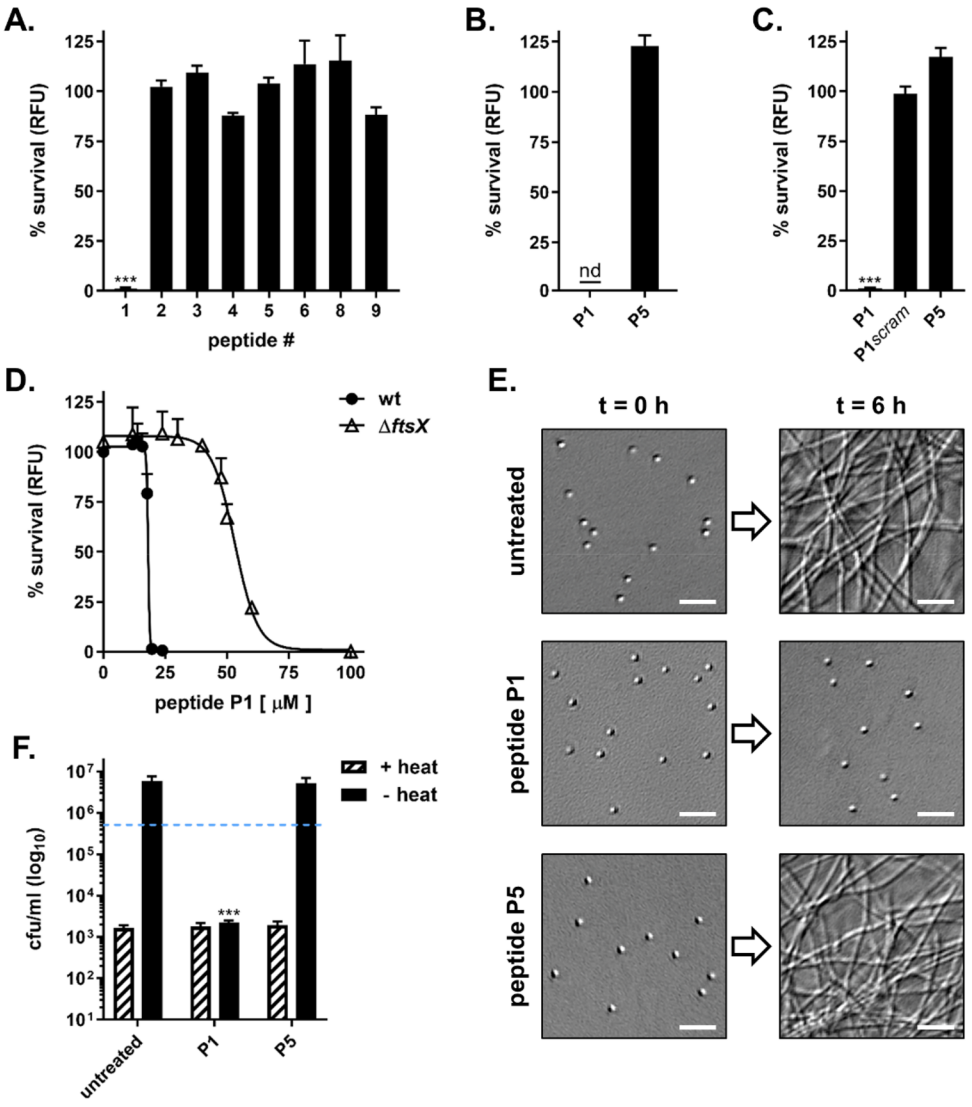

Figure 2. Antimicrobial effects of CXCL10-derived peptides against *Bacillus* spp. (A) *B. anthracis* Sterne 7702 and (B) *B. subtilis* 168 bacilli were exposed to 50 μM of the indicated peptide, or (C) *B. anthracis* was treated with a sequence-scrambled peptide P1 variant (P1*scram*; TISVCPTLRRIVSC), in cell-culture medium that contains physiologic levels of salt (i.e., DMEM) + 10% FBS for 4 h. Bacterial survival was then measured using the fluorescent viability reagent alamarBlue. Data are expressed as a percentage of the untreated control (relative fluorescence unit, RFU) and report the mean ± standard deviation (SD) of $n = 3$ experiments; nd = none detected. ***$p < 0.001$ as compared to peptide P5 by one-way ANOVA with Dunnett's multiple comparisons test. (D) Wild-type (wt) and Δ*ftsX B. anthracis* bacilli were exposed to increasing concentrations of peptide P1 and bacterial viability was measured as above; $n = 3$ experiments. Fitted curves were generated by nonlinear regression (sigmoidal dose−response, variable-slope equation) and used to calculate the EC_{50} ± 95% confidence interval for peptide P1 against each *B. anthracis* strain examined: wild-type (EC_{50} = 18.1 ± 0.3 μM; R^2 = 0.99) and Δ*ftsX* (EC_{50} = 53.1 ± 0.8 μM; R^2 = 0.97). (E) *B. anthracis* Sterne 7702 spores were exposed to buffer alone (untreated control) or 50 μM of the indicated peptide in RPMI medium +5% FBS. Spore germination and the subsequent outgrowth of vegetative bacilli were assessed using light microscopy. Representative photomicrographs from >12 fields ($n = 3$ experiments) are shown at 500× magnification for the $t = 0$ and 6 h time points; scale bar = 10 μm. Expanded field-of-view images are shown in Figure S1. (F) The viability of *B. anthracis* spores, treated as described above, was quantified at 0 and 6 h using cfu determination ± heat treatment to distinguish heat-resistant spores from heat-sensitive germinating organisms and bacilli. The initial spore inoculum is displayed as a dotted line (---). Data are expressed as cfu/mL (log_{10}) and report the mean ± SD. A representative data set from $n = 4$ experiments is shown. ***$p < 0.001$ as compared to the respective untreated control by one-way ANOVA with Dunnett's multiple comparisons test.

than 10-fold (due to the outgrowth of vegetative bacilli). In contrast, 6 h cfu counts from peptide P1-treated spores with and without heat treatment were equivalent (indicating few, if any, germinated organisms), and recovered viable spores were less than 1% of the initial inoculum. These findings, together with the visible lack of cytological changes by peptide P1-treated spores, suggest that peptide P1 prevents spore germination and reduces spore viability.

Bactericidal Effects of CXCL10-Derived Peptides against Carbapenem-Resistant *Klebsiella pneumoniae*. Peptides comprising the CXCL10-derived peptide library were evaluated for their capacity to kill the Gram-negative *K. pneumoniae* clinical isolate BL13802, a carbapenem-resistant MDR pathogen that produces both the New Delhi metallo-beta-lactamase (NDM)-1 and oxacillinase (OXA)-48 carbapenemase enzymes.[18] Peptide susceptibility was evaluated under two sets of conditions: (i) a low-salt, hypotonic medium used

https://doi.org/10.1021/acsinfecdis.2c00456
ACS Infect. Dis. 2023, 9, 122−139

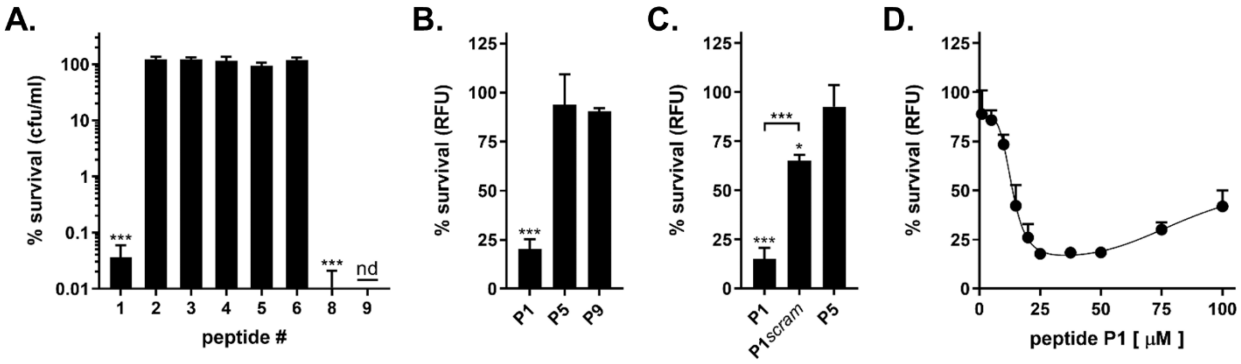

Figure 3. Bactericidal effects of CXCL10-derived peptides against MDR *K. pneumoniae*. (A) *K. pneumoniae* BL13802 was exposed to 5.6 μM of the indicated peptide in Kph buffer + 1% TSB for 2 h. Bacterial survival was measured by cfu determination. Data are expressed as a percentage of the untreated control (log_{10}) and report the mean ± SD of $n = 3$ experiments. (B, C) *K. pneumoniae* BL13802 was exposed to 50 μM of the indicated peptide, or sequence-scrambled variant (P1*scram*), in RPMI medium. Bacterial survival was measured using the fluorescent viability reagent alamarBlue. Data are expressed as a percentage of the untreated control (RFU) and report the mean ± SD of $n = 3$ experiments; nd = none detected. ***$p < 0.001$ and *$p < 0.05$ as compared to peptide P5, or between specified groups, by one-way ANOVA with Tukey's multiple comparisons test. (D) *K. pneumoniae* BL13802 was exposed to increasing concentrations of peptide P1 and bacterial viability was measured using alamarBlue; $n = 4$ experiments. Nonlinear regression (bell-shaped equation) was used to calculate the EC_{50} ± 95% confidence interval for peptide P1 (EC_{50} = 13.4 ± 1.2 μM; $R^2 = 0.95$).

previously to screen chemokines and other host effectors for antimicrobial effects (i.e., 10 mM potassium phosphate buffer supplemented with 1% tryptic soy broth; Kph buffer + 1% TSB),[5,18,27] and (ii) a cell-culture medium containing physiologic levels of salts (i.e., RPMI medium). In Kph buffer + 1% TSB, peptides derived from either the N-terminus (peptide P1) or C-terminus (peptides P8 and P9) of CXCL10 efficiently killed *K. pneumoniae* as shown by cfu determination (Figure 3A). In RPMI medium, peptide P1 retained significant bactericidal activity; however, these conditions abolished the ability of the C-terminal peptide derivative P9 to kill *K. pneumoniae* (Figure 3B).

The antimicrobial effects of peptide P1 against MDR *K. pneumoniae* were sequence specific (Figure 3C), although the scrambled peptide variant did exhibit some killing activity. Since it can be challenging to extensively disrupt the physicochemical properties of short peptides by rearranging their amino acid constituents, as is the case here, CXCL10-derived peptide P5 (a cationic peptide that was not observed to kill any bacterial species under any condition examined in this research) was included in these and following experiments as a negative, peptide-treated control. The killing of *K. pneumoniae* BL13802 by peptide P1 was also concentration dependent (EC_{50} of 13.4 ± 1.2 μM; Figure 3D). Of note, despite being soluble at 5 mM or more in dH_2O, peptide P1 concentrations greater than ∼50 μM in RPMI medium resulted in increasing precipitation and progressively diminished bactericidal activity.

Killing of Diverse Antibiotic-Resistant Pathogens by Peptides P1 and P9. To evaluate the spectrum of activity for antimicrobial CXCL10-derived peptides, clinically challenging pathogens including Gram-negative bacteria (carbapenem-resistant, XDR isolates of *Acinetobacter baumannii*, *Pseudomonas aeruginosa*, and *Enterobacter cloacae*; ceftriaxone-resistant, MDR isolates of *Salmonella enterica* serovar Typhi and *Shigella flexneri*), as well as Gram-positive bacteria (vancomycin-resistant *Enterococcus faecium*, VRE; methicillin-resistant *Staphylococcus aureus*, MRSA), were exposed to peptide P1, P9, or the P5 negative-control in Kph buffer + 1% TSB (Figure 4A) and RPMI medium (Figure 4B). In low-salt Kph buffer + 1% TSB, peptide P1 reduced the viability of each pathogen tested by ∼100-fold or more. In matched analyses, peptide P9 mediated substantial killing of Gram-negative bacterial species, except *E. cloacae*, but had little to no effect on the viability of Gram-positive organisms. In RPMI medium containing physiologic levels of salts, peptide P1 retained significant bactericidal activity against *A. baumannii*, *E. cloacae*, *Salmonella* Typhi , *E. faecium*, and *S. aureus*. In contrast, peptide P9 lost its capacity to kill any of the isolates examined.

The potential of CXCL10-derived peptides to kill the fastidious Gram-negative pathogen *Neisseria gonorrhoeae* was also evaluated (Figure 4C), using the organism-specific gonococcal base liquid (GCBL) medium with Kellogg's supplements.[28] In these experiments, two clinical isolates of *N. gonorrhoeae* were assayed: FA1090 (a strain susceptible to the current recommended treatment ceftriaxone) and H041 (a ceftriaxone-resistant, XDR isolate). Peptide P1 was found to exert significant bactericidal effects against *N. gonorrhoeae* regardless of the strain's particular antibiotic-resistance profile. Peptide P9 also killed each isolate examined; however, reductions in bacterial viability were more modest.

Absence of Cross-Resistance between Colistin and CXCL10-Derived Peptides. Colistin is a cationic, lipopeptide antibiotic that targets bacteria through electrostatic interactions with the anionic phosphate groups present on the lipid A component of lipopolysaccharide (LPS),[29,30] a major constituent of the outer membrane of Gram-negative bacteria. Chemical modification of these phosphate groups abates the negative charge of the bacterial cell envelope, prevents colistin from localizing to its site of action, and confers resistance against this antibiotic. Since analogous charge-based interactions also underpin the activity of other antimicrobials, colistin-resistant organisms may be less susceptible to other bactericidal agents.[31] Therefore, we evaluated whether colistin-resistant bacterial strains exhibit cross-resistance against CXCL10-derived peptides.

Likely the most concerning determinants of colistin resistance are mobilized colistin resistance (*mcr*) genes, plasmid-based loci which encode phosphoethanolamine transferase enzymes that catalyze the addition of phosphoethanolamine (pEtN) onto the phosphate groups of lipid A and thereby replace anionic phosphates with cationic amines.[29]

https://doi.org/10.1021/acsinfecdis.2c00456
ACS Infect. Dis. 2023, 9, 122−139

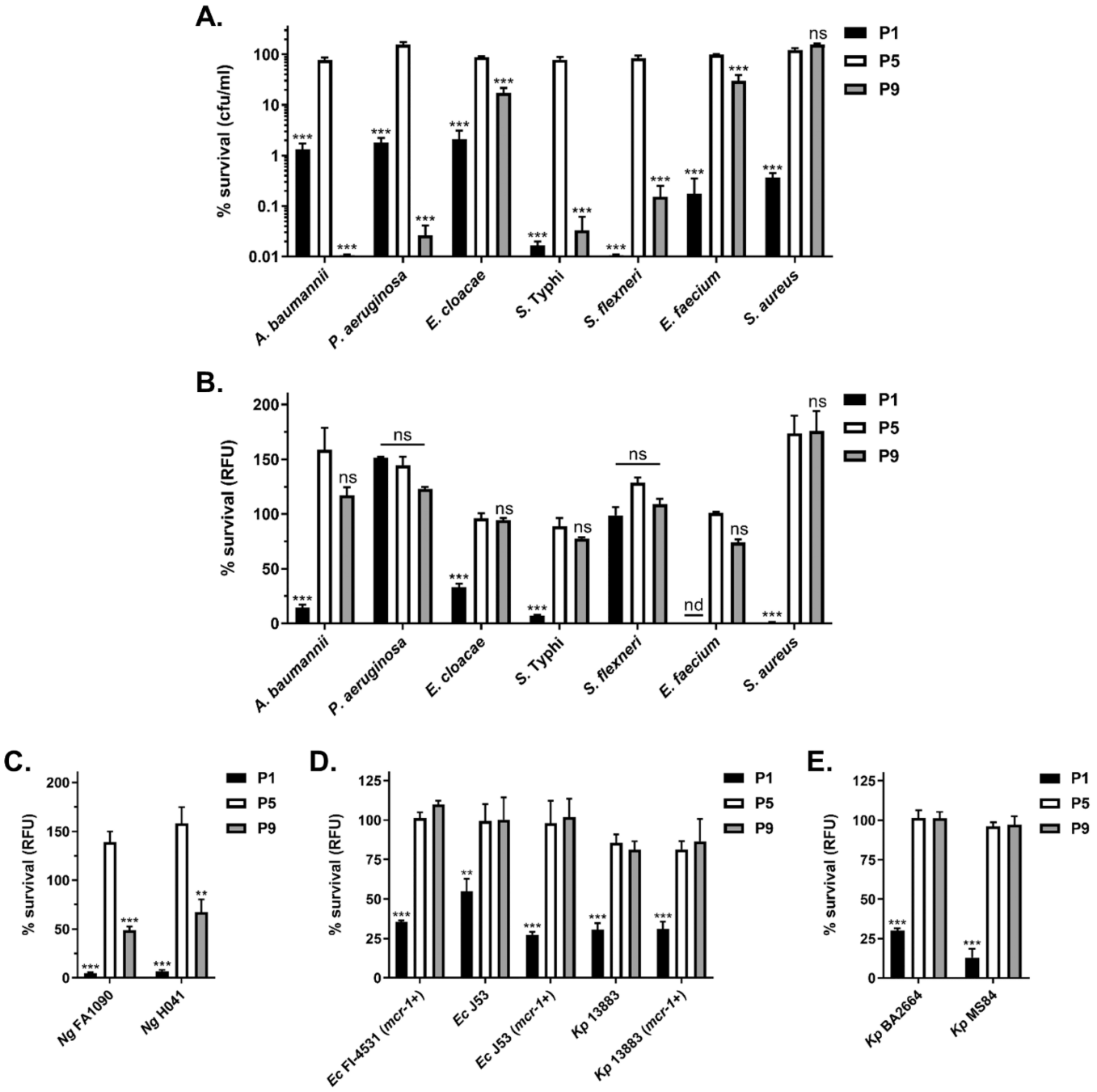

Figure 4. Antimicrobial effects of peptides P1 and P9 against diverse antibiotic-resistant bacterial pathogens. Gram-negative bacteria (*A. baumannii* AR0304, *P. aeruginosa* AR0231, *E. cloacae* BL36213, *S. enterica* serovar Typhi BL31130, *S. flexneri* BL28504) and Gram-positive bacteria (*E. faecium* AR0575, *S. aureus* LAC) were exposed to (A) 5.6 μM of peptide P1, P5, or P9 in Kph buffer + 1% TSB for 2 h prior to cfu determination or (B) 50 μM of peptide P1, P5, or P9 in RPMI medium for 2 h prior to alamarBlue analysis. (C) *N. gonorrhoeae* (*Ng*) strains FA1090 and H041 were exposed to 50 μM of the indicated peptide in 0.2× GCBL medium for 3 h prior to alamarBlue analysis. (D) *E. coli* (*Ec*) clinical isolate FI-4531 and strain J53 or *K. pneumoniae* (*Kp*) strain 13883 (with or without the plasmid-encoded colistin resistance determinant *mcr-1*), as well as (E) colistin-resistant *Kp* isolates BA2664 and MS84 (that harbor genetic alterations of *pmrB* or *mgrB*, respectively), were exposed to 50 μM of peptide P1, P5, or P9 in RPMI medium for 2 h prior to alamarBlue analysis. In all panels, data are expressed as a percentage of the untreated control and report the mean ± SD of $n = 3$ experiments; nd = none detected. ***$p < 0.001$ and **$p < 0.01$ as compared to peptide P5 by one-way ANOVA with Dunnett's multiple comparisons test; ns = not significant.

The ability of CXCL10-derived peptides P1 and P9 to kill colistin-resistant, *mcr-1*-positive bacterial strains was evaluated using the *E. coli* clinical isolate FI-4531 that expresses *mcr-1*, and also pairs of isogenic *E. coli* and *K. pneumoniae* strains that do, or do not, harbor *mcr-1* (Figure 4D). Peptide P1 was found to kill each *mcr-1*-positive strain tested; these bactericidal effects were greater than or equal to those observed against matched, colistin-susceptible strains. As expected due to the inability of peptide P9 to exert antimicrobial activity in physiologic medium, the viability of peptide P9-treated bacteria was undiminished and equivalent to that of organisms exposed to the peptide P5 negative control.

https://doi.org/10.1021/acsinfecdis.2c00456
ACS Infect. Dis. 2023, 9, 122−139

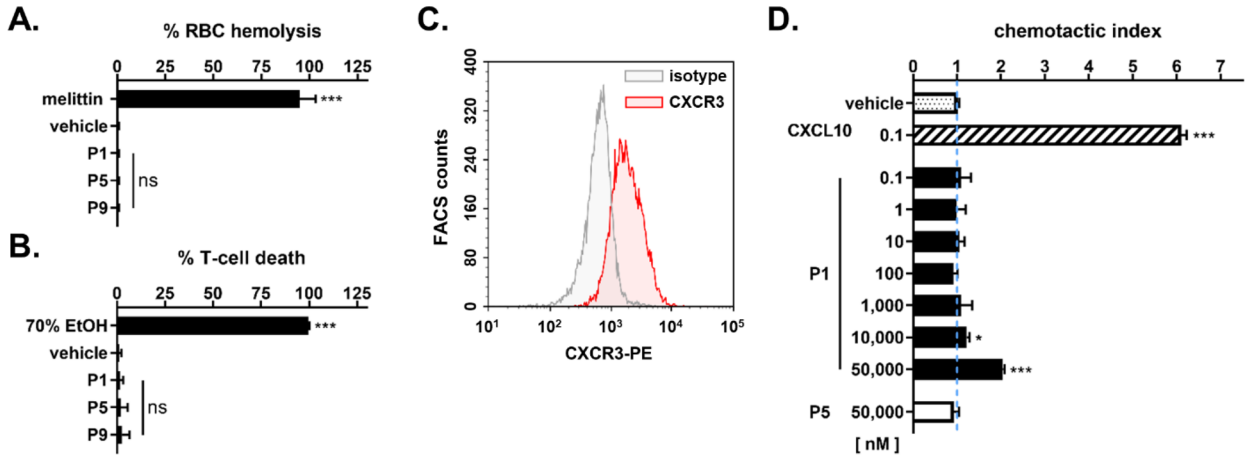

Figure 5. Hemolytic, cytotoxic, and chemotactic activities of peptides P1 and P9. (A) Human RBCs were exposed to 50 μM of the indicated peptide, vehicle alone (dH_2O), or 8 μM of the membrane-permeabilizing peptide melittin (positive control) in RPMI medium with 1% BSA and without phenol red for 1 h. Hemolysis was determined using spectrophotometry (540 nm); data are expressed as a percentage of the fully hemolyzed control (1% Triton X-100). (B) Human T-cells were exposed to peptide P1, P5, or P9 (50 μM), vehicle alone, or 70% ethanol (EtOH) in RPMI medium + 1% BSA for 2 h. Cell viability was measured by LIVE/DEAD staining. Data are expressed as the percentage of dead cells. (C) Surface expression of CXCR3 on CD3/CD28-stimulated human T-cells as determined using flow cytometry. Histograms show the fluorescence intensities of singlet, $CD45^+$ cells stained with phycoerythrin (PE)-conjugated anti-CXCR3 (red) or isotype control (gray) antibodies. CXCR3 expression on $CD4^+$ and $CD8^+$ T-cell subsets are presented in Figure S2. (D) Migration of CXCR3-expressing human T-cells in response to vehicle-alone, full-length human CXCL10 (0.1 nM), or the indicated concentration(s) of peptide P1 or P5. Data are expressed as chemotactic index (migrated cells in treatment group/migrated cells in buffer-only control); a chemotactic index greater than 1 (dashed line, ---) indicates chemoattraction. Panels A, B, and D report the mean ± SD from $n = 3-4$ donors; panel C shows representative plots from $n = 3$ donors. ***$p < 0.001$ and *$p < 0.05$ as compared to the vehicle-alone control by one-way ANOVA with Dunnett's multiple comparisons test; ns = not significant.

In addition to mobile determinants, colistin resistance can also arise from chromosomal mutations that dysregulate the regulatory networks governing LPS modification. Major examples include point mutations among genes encoding the two-component systems PmrA/B and PhoP/Q, or genetic disruption of MgrB (a negative regulator of PhoP/Q signaling), that lead to the constitutive expression of enzymes that synthesize 4-amino-4-deoxy-L-arabinose (L-Ara4N) and catalyze its addition to the phosphate groups of lipid A.[29] Like pEtN addition, this modification reduces the capacity of colistin to target and kill bacteria. Peptide P1, but not peptide P9, killed colistin-resistant *K. pneumoniae* clinical isolates having a mutated *pmrB* gene (strain BA2664) or a disrupted *mgrB* locus (strain MS84) (Figure 4E).[18] That peptide P1 is able to kill colistin-resistant pathogens with pEtN- or L-Ara4N modified lipid A demonstrates an absence of cross-resistance, and suggests charged-based interactions with the cell envelope are not essential to peptide P1-mediated antimicrobial activity.

Host-Targeted Effects of CXCL10-Derived Peptides. To identify potential cytotoxic effects exerted by peptide P1 or P9, experiments measuring human red blood cell (RBC) hemolysis (Figure 5A) and T-cell viability (Figure 5B) were conducted. Hemolysis was evaluated in RPMI medium with 1% bovine serum albumin (BSA) and without phenol red, using spectrometry to quantify the release of hemoglobin from lysed cells. Melittin, a 26-residue cytolytic peptide, was used as a positive control and was observed to cause high levels of hemolysis. RBCs treated with bactericidal concentrations of peptide P1 or P9, as well as those exposed to peptide P5 or vehicle-alone (dH_2O), demonstrated negligible hemolysis. The viability of primary human T-cells was measured by fluorescence-based LIVE/DEAD staining in RPMI medium with 1% BSA. Exposure of T cells to 70% ethanol (positive control) was found to eliminate nearly all viable cells. In contrast, peptides P1, P5, and P9 were each well tolerated by T cells, with cellular viability equivalent to that of vehicle-alone (less than 5% cell death). Thus, under the conditions tested, CXCL10-derived peptides were not observed to kill primary human cells.

The N-terminus and N-loop region of CXCL10 contain many of the amino acid residues important for binding to, and activating, the cellular chemokine-receptor CXCR3 that functions in immune-cell recruitment.[9,32−34] Several determinants critical to triggering receptor signaling (i.e., arginine-5, valine-7, and especially arginine-8) precede the first conserved cysteine residue and are contained in peptide P1. To investigate the possibility that peptide P1 is chemotactic, CXCR3-expressing human T-cells were prepared via CD3/CD28 stimulation (Figures 5C and S2), and then used in ChemoTx cellular-migration assays (Figure 5D). Full-length human CXCL10 was used as a positive control and at a concentration of 0.1 nM, which elicits a clear effect across donors in this experimental system (Figure S3), produced a chemotactic index (CI) of approximately 6 (meaning ~6-fold more cells migrated in response to CXCL10 than to buffer-alone). Peptide P1 did not exhibit chemotactic activity at concentrations commensurate to CXCL10; however, at bactericidal concentrations (e.g., 50 μM), peptide P1 induced moderate levels of chemotaxis (CI of ~2). Matched micromolar-levels of peptide P5, which contains the central 40's loop that stabilizes the interaction of CXCL10 with CXCR3,[32,34] did not elicit T-cell migration. In sum, although the chemotactic effect of peptide P1 appears specific to this N-terminal derivative, a large excess of peptide is needed to induce cellular migration as compared to the full-length CXCL10 protein.

Analysis of Peptide P1 and P9 Secondary Structure. Since peptide secondary structure can be a decisive factor in antimicrobial activity, the principal structural elements of peptide P1 (Figure 6A) and P9 (Figure 6B) were determined

https://doi.org/10.1021/acsinfecdis.2c00456
ACS Infect. Dis. 2023, 9, 122−139

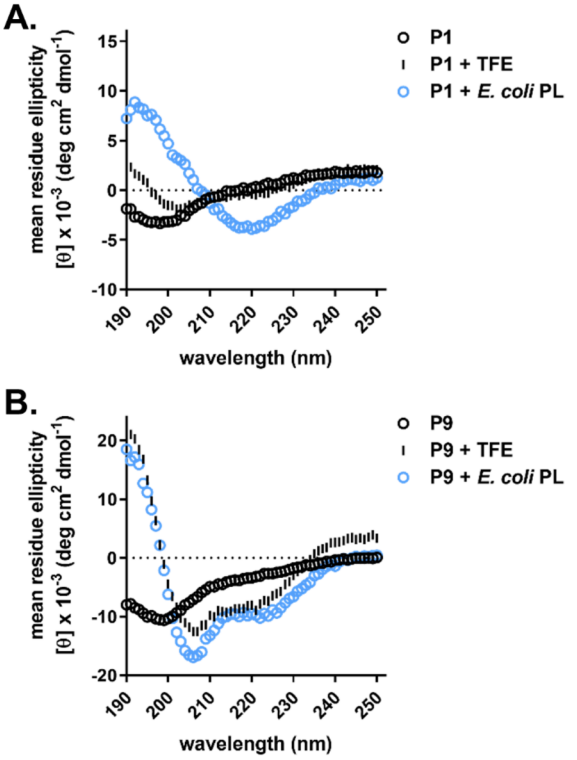

Figure 6. Determination of peptide secondary structure. CD spectra of peptide P1 (A) and P9 (B) were obtained at 25 °C following pre-incubation (1 h at 37 °C) with Kph buffer-only, 50% TFE, or 800 μM of liposomes prepared from *E. coli* polar lipids (PL). Data are expressed as mean residue ellipticity and report the mean of $n = 3-4$ scans. Solvent/reagent controls were measured in parallel and are presented in Figure S4.

using circular dichroism (CD) spectroscopy in three environments: (i) Kph buffer-only, as well as buffer with (ii) 50% 2,2,2-trifluoroethanol (TFE; an organic solvent that promotes and stabilizes the formation of secondary structures, especially α-helices[35]) or (iii) liposomes prepared from *E. coli* polar lipids (a mimetic of Gram-negative bacterial membranes). Solvent/reagent controls without peptide generated little or no CD signal between 190 and 250 nm (Figure S4).

Peptide P1 is mostly derived from the unstructured N-terminal region of CXCL10. Expectantly, the CD spectrum of peptide P1 in Kph buffer resembled that of a disordered/unstructured random coil (negative peak at 196 nm and low ellipticity above 210 nm). No regular secondary structure was evident for peptide P1 in 50% TFE either. In contrast, when exposed to liposomes that mimic bacterial membranes, the spectrum of peptide P1 shifted considerably and exhibited characteristics typical of β-sheet structure (positive peak at 192 nm, negative peak at 220 nm). Spectral analysis using BeStSel, a structure determination and fold recognition Web server,[36] estimated that in this membrane-mimetic environment, the secondary structure content of peptide P1 was predominately antiparallel β-sheet (60%) and turn (12%).

The majority of peptide P9 corresponds to the C-terminal α-helix of CXCL10, yet this native conformation was not observed by CD spectroscopy for peptide P9 in Kph buffer. Rather, the spectrum of peptide P9 in buffer alone matched that of a random coil. In contrast, α-helical secondary structure was evident in the CD spectra of peptide P9 in 50% TFE and, even more so, in the presence of liposomes prepared from *E. coli* polar lipids (positive peak at 190 nm, negative peaks at 206 and 222 nm). BeStSel analysis of the latter peptide P9 spectrum estimated α-helix (35%) to be the main element of secondary structure, though turn (18%) and antiparallel β-sheet (12%) features were also predicted.

Stabilizing the α-Helicity of Peptide P9 through Hydrocarbon Stapling. Although derived from the α-helical C-terminus of CXCL10, CD spectroscopy shows that peptide P9 requires a particularly conducive environment (e.g., TFE, bacterial membrane mimetics) in order to adopt this native conformation. Perhaps analogously, peptide P9 exerts bactericidal effects only against Gram-negative bacteria in low-salt medium—conditions that generally favor α-helicity.[37,38] Indeed, physiologic levels of salts are well known to diminish the antimicrobial effects of many α-helical peptides, presumably owing to the disruption of molecular forces that underpin conformational stability (e.g., hydrogen bonding, electrostatic ion-pair interactions).[39−41] Toward promoting the α-helical secondary structure of peptide P9, and thereby possibly enhancing the antimicrobial actions of this peptide, we pursued a chemical approach in which a pair of alkene-bearing unnatural amino acids are inserted, and then coupled by metathesis, to form a stabilizing hydrocarbon brace or "staple" along one face of the α-helix.[42]

To identify the amino acid residues of peptide P9 that could potentially be replaced by those amenable to hydrocarbon stapling, we generated an alanine-scan library of peptide P9 variants and tested these peptides for bactericidal effects against *K. pneumoniae* in low-salt medium (Figure 7A). Among the amino acids that could be replaced without reducing bacterial killing under these permissive conditions was asparagine-8. Advantageously, this residue is separated from alanine-12 by four positions, which is ideal spacing for generating a single-turn staple.[42] To this end, the native residues at positions 8 and 12 of peptide P9 were substituted with alkene-bearing (*S*)-pentenyl alanine (S5A) residues that were then stapled via ring-closing metathesis using Grubbs' first-generation catalyst (Figure S5A). Analytical high-performance liquid chromatography (HPLC) and matrix-assisted laser desorption/ionization (MALDI) time-of-flight (TOF) mass spectrometry were used to confirm the successful installation of the staple (Figure S5B,C). Representations of CXCL10-derived peptide P9, as well as the pre-stapled and stapled peptide variants, are presented in Figure 7B; corresponding helical-wheel diagrams that indicate the relative positions of amino acid residues are shown in Figure S6.

The effects of unnatural amino acid substitutions and stapling on the secondary structure of peptide P9 were determined using CD spectroscopy (Figure 7C). In contrast to the spectrum obtained from unmodified peptide P9 in buffer alone, which corresponded to a random-coil conformation, the spectra for pre-stapled and stapled peptide P9 were consistent with α-helical secondary structure. In particular, stapled peptide P9 had negative peaks at 206 and 222 nm that exceeded those for either the pre-stapled peptide or unmodified peptide P9 in the presence of 50% TFE. As a measure of α-helix stability, melting curves were generated at 222 nm for the P9 series of peptides (Figure 7D). The negative peak at 222 nm for both pre-stapled and stapled peptide P9 diminished only slightly as temperature increased. That no abrupt and significant loss of signal was observed suggests that each peptide variant was generally stable against thermal denaturation. Full-spectrum scans following heating then

https://doi.org/10.1021/acsinfecdis.2c00456
ACS Infect. Dis. 2023, 9, 122−139

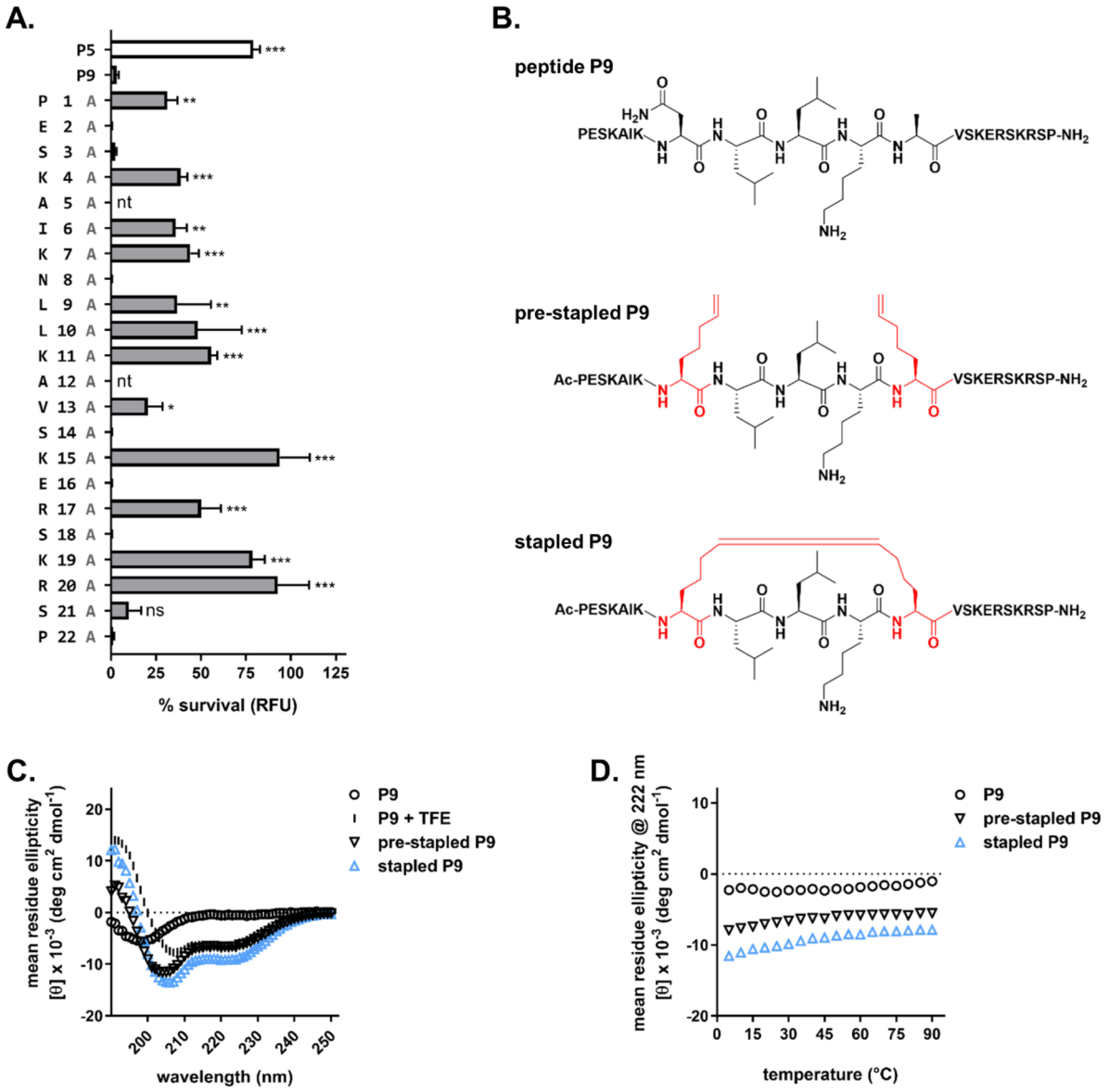

Figure 7. Design and derivation of stapled peptide P9. (A) Alanine scan of peptide P9. *K. pneumoniae* BL13802 was exposed to 5.6 μM of individual variant peptides, each containing a single alanine substitution at the designated position, in Kph buffer + 1% TSB for 2 h. Individual samples were then combined 1:1 with 2× LB medium and bacterial survival was measured by alamarBlue analysis The 22 amino acid native sequence of peptide P9 is indicated in black text (left); positions already containing an alanine were not tested (nt). Data are expressed as a percentage of the untreated control (RFU) and report the mean ± SD of n = 3−4 experiments. ***p < 0.001, **p < 0.01, and *p < 0.05 as compared to peptide P5 by one-way ANOVA with Dunnett's multiple comparisons test; ns = not significant. (B) Representations of unmodified (top), pre-stapled (middle), and stapled (bottom) peptide P9. Substitutions with (S5A) residues at positions 8 and 12 are marked in red; Ac = N-terminal acetylation, NH_2 = C-terminal amidation. (C) CD spectra of peptide P9 ± 50% TFE, as well as pre-stapled and stapled peptide P9 in 10 mM phosphate-buffered saline (PBS; 40 μM peptide at 25 °C). Data are expressed as mean residue ellipticity and report the mean of n = 3−4 scans. (D) Single-wavelength (222 nm) melting curves obtained from the indicated P9 series peptide (40 μM peptide, 5 to 95 °C at 5 °C/min). Data are expressed as mean residue ellipticity and report the mean of n = 3−4 scans.

cooling, demonstrated that minor losses in secondary structure were reversible (Figure S7).

Antimicrobial Effects of Stapled Peptide P9 against Bacterial Pathogens. By stabilizing the α-helical secondary structure of peptide P9, we expected to improve the capacity of this peptide to kill bacteria under physiologic conditions. Indeed, unlike peptide P9 (Figure 2A), both pre-stapled and stapled peptide P9 were found to exert bactericidal activity against *B. anthracis* vegetative bacilli in tissue-culture medium with serum (Figure 8A). These effects were concentration dependent with EC_{50} values of ∼4−5 μM, and killing was similar against Δ*ftsX B. anthracis* bacilli. In contrast to peptide P9, both α-helical variants prevented *B. anthracis* spore germination and vegetative outgrowth as determined by light microscopy (Figures 8B and S8). Viability determination ± heat treatment also indicated reduced spore germination 6 h following peptide exposure, as well as modest reductions in the viability of ungerminated spores as compared to the initial inoculum (Figure 8C).

The bactericidal effects of pre-stapled and stapled peptide P9 were also assessed against antibiotic-resistant clinical isolates representing a diverse range of pathogenic bacterial species

https://doi.org/10.1021/acsinfecdis.2c00456
ACS Infect. Dis. 2023, 9, 122−139

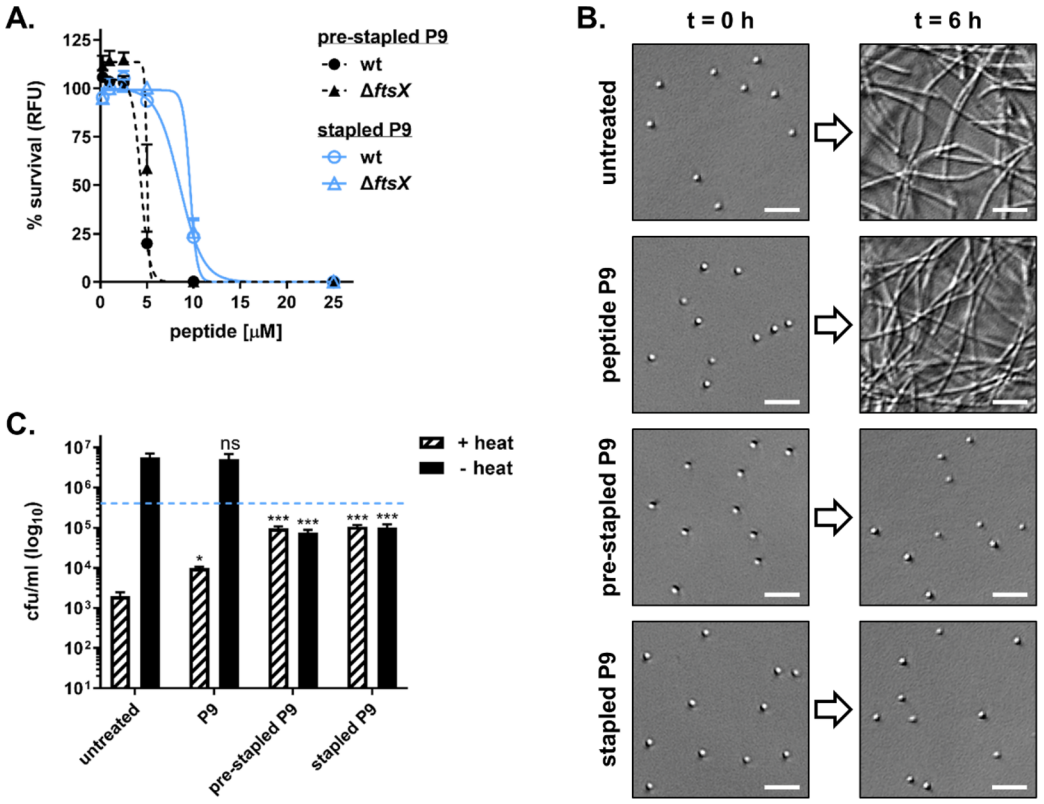

Figure 8. Antimicrobial effects of P9 series peptides against *B. anthracis*. (A) wt and Δ*ftsX B. anthracis* bacilli were exposed to increasing concentrations of pre-stapled and stapled peptide P9 in DMEM + 10% FBS for 4 h. Bacterial survival was measured using alamarBlue. Data are expressed as a percentage of the untreated control (RFU) and report the mean ± SD of $n = 3$ experiments. Fitted curves were generated by nonlinear regression (sigmoidal dose−response, variable-slope equation) and used to calculate the EC_{50} ± 95% confidence interval for both peptides against each *B. anthracis* strain examined: wt + pre-stapled P9 ($EC_{50} = 4.3 \pm 0.4$ μM; $R^2 = 0.99$), Δ*ftsX* + pre-stapled P9 ($EC_{50} = 5.0 \pm 1.2$ μM; $R^2 = 0.96$), wt + stapled P9 ($EC_{50} = 8.5 \pm 0.9$ μM; $R^2 = 0.96$), Δ*ftsX* + stapled P9 ($EC_{50} = 9.6 \pm 1.0$ μM; $R^2 = 0.97$). (B) Photomicrographs of *B. anthracis* spores exposed to buffer-only (untreated control) or 50 μM of the indicated peptide in RPMI medium +5% FBS. Representative images from >12 fields ($n = 3$ experiments) are shown at 500× magnification for the $t = 0$ and 6 h time points; scale bar = 10 μm. Expanded fields of view are shown in Figure S8. (C) The viability of *B. anthracis* at 6 h following peptide exposure was quantified using cfu determination ± heat treatment to distinguish heat-resistant spores from heat-sensitive germinating organisms and bacilli; the initial spore inoculum is displayed as a dotted line (---). Data are expressed as cfu/mL (log_{10}) and report the mean ± SD. A representative data set from $n = 4$ experiments is shown. ***$p < 0.001$ and *$p < 0.05$ as compared to the respective untreated control by one-way ANOVA with Dunnett's multiple comparisons test.

(Figure 9A). Each of the α-helical peptide P9 variants exhibited antimicrobial activity against both Gram-positive and Gram-negative organisms in tissue-culture medium—a marked improvement over unmodified peptide P9. XDR *A. baumannii*, VRE, MRSA, and *N. gonorrhoeae* were observed to be particularly susceptible to these peptide-mediated actions. Conversely, the viability of *P. aeruginosa* was not affected by any P9 series peptide tested. This observation may reflect the extensive arsenal of proteases secreted by *P. aeruginosa*, which includes enzymes previously found to target host chemokines.[43]

Pre-stapled and stapled peptide P9 also killed colistin-resistant *K. pneumoniae* and *E. coli* strains (Figure 9B,C, including strains that harbor plasmid-based *mcr* genes (Figure 9C). Generally, the bactericidal effects of pre-stapled and stapled peptide P9 were equivalent; however, in some instances (e.g., *S. flexneri*, *K. pneumoniae* MS84) the pre-stapled variant outperformed stapled P9. Regarding eukaryotic-cell viability, neither pre-stapled nor stapled peptide P9 exerted hemolytic effects against human RBCs (Figure 9D). These peptides were less well tolerated by primary T-cells. Specifically, in RPMI medium with 1% BSA, pre-stapled and stapled peptide P9 killed approximately 75% and 45% of treated cells, respectively (Figure 9E, left). In X-VIVO 15, a serum-free hematopoietic cell medium, these cytotoxic effects were greatly reduced (Figure 9E, right). Irrespective of the culture medium, the pre-stapled variant exerted significantly more cytotoxicity than stapled peptide P9.

DISCUSSION

The chemokine CXCL10 is a central mediator in host defense against infectious diseases.[1,44] While the molecular features responsible for eliciting receptor-dependent actions such as immune-cell migration and activation are increasingly well understood,[9,32,34] the determinants of CXCL10-mediated antimicrobial effects have not been previously identified. In this study, using peptide-based mapping and structure/function analyses, we discovered two discrete and unalike domains in the N- and C-terminal regions of human CXCL10 that kill bacteria. Peptides derived from each of these domains exerted broad-spectrum antimicrobial activity against diverse Gram-positive and Gram-negative bacterial species, including organisms identified by the CDC as urgent (e.g., carbapenem-resistant *Acinetobacter* and *Enterobacteriaceae*) or serious (e.g., MRSA, VRE, and drug-resistant *Salmonella*) antibiotic-resistance threats.[17] Our findings provide new insight into

https://doi.org/10.1021/acsinfecdis.2c00456
ACS Infect. Dis. 2023, 9, 122−139

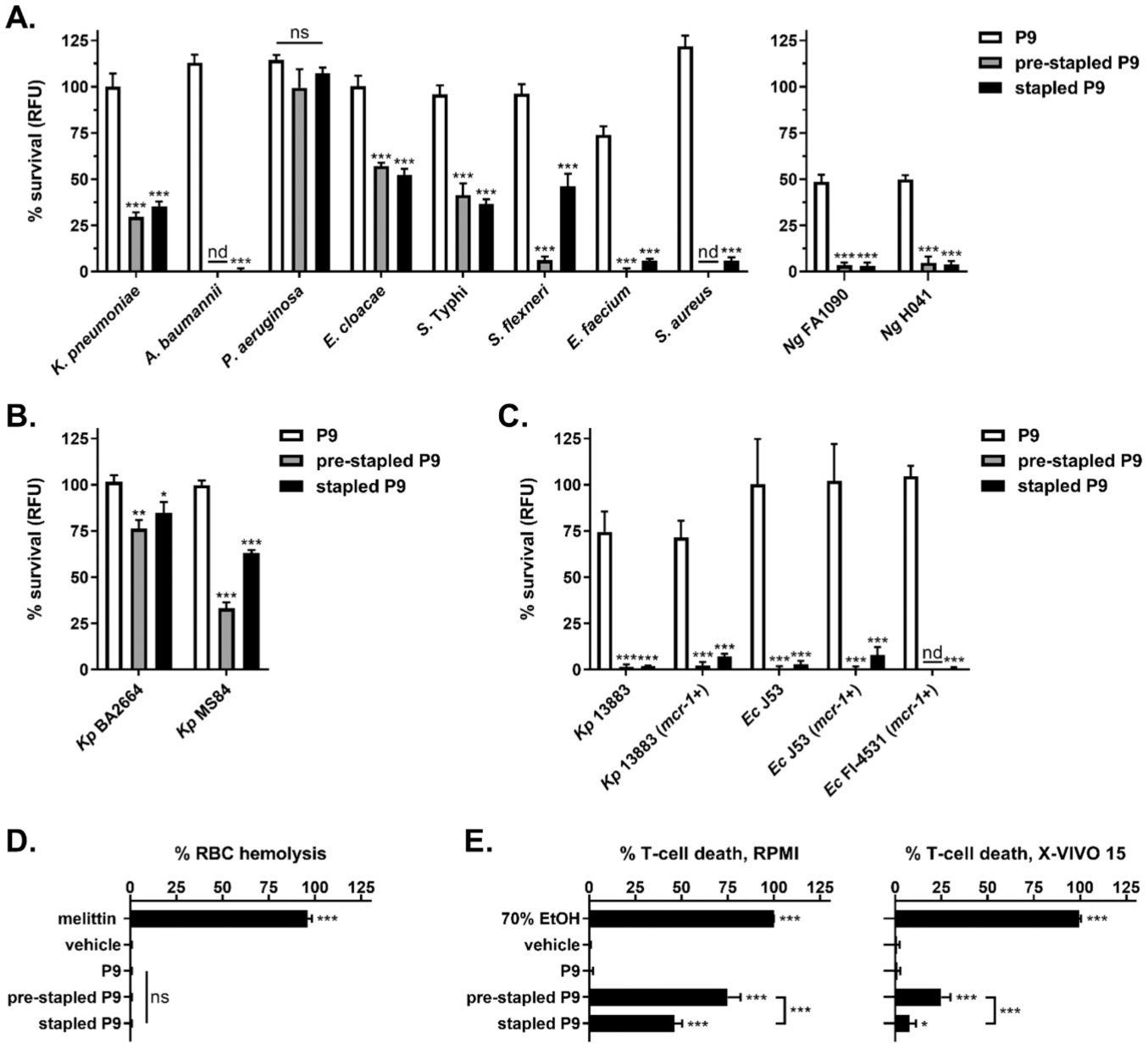

Figure 9. Pathogen- and host-targeted activities of P9 series peptides. (A) Gram-negative (*K. pneumoniae* BL13802, *A. baumannii* AR0304, *P. aeruginosa* AR0231, *E. cloacae* BL36213, *S. enterica* serovar Typhi BL31130, *S. flexneri* BL28504) and Gram-positive (*E. faecium* AR0575, *S. aureus* LAC) antibiotic-resistant clinical isolates were exposed to 50 μM of unmodified, pre-stapled, or stapled peptide P9 in RPMI medium for 2 h. The Gram-negative pathogen *N. gonorrhoeae* (*Ng*; strain FA1090 and XDR clinical isolate H041) was also treated with P9 series peptides, but in 0.2× GCBL medium for 3 h. (B) Colistin-resistant *K. pneumoniae* (*Kp*) isolates BA2664 and MS84, as well as (C) *E. coli* (*Ec*) clinical isolate FI-4531 and strain J53 or *Kp* strain 13883 (with or without the plasmid-encoded colistin resistance determinant *mcr-1*), were exposed to 50 μM of the indicated peptide in RPMI medium for 2 h. Bacterial viability was measured by alamarBlue analysis. Killing data are expressed as a percentage of the untreated control (RFU) and report the mean ± SD of n = 3−4 experiments; nd = none detected. ***p < 0.001, **p < 0.01, and *p < 0.05 as compared to unmodified peptide P9 by one-way ANOVA with Dunnett's multiple comparisons test; ns = not significant. (D) Human RBCs were exposed to the indicated peptide (50 μM), vehicle alone (dH_2O), or the positive control melittin (8 μM) in RPMI medium + 1% BSA for 1 h. Hemolysis was determined using spectrophotometry (540 nm). Data are expressed as a percentage of the fully hemolyzed control (1% Triton X-100) and report the mean ± SD from n = 3 donors. (E) Viability of CXCR3-expressing human T-cells as measured by LIVE/DEAD staining following a 2 h exposure to the indicated peptide (50 μM), vehicle alone (dH_2O), or 70% ethanol (EtOH) in RPMI medium + 1% BSA (left) or X-VIVO 15 medium (right). Data are expressed as the percentage of dead cells and report the mean ± SD from n = 3 donors. ***p < 0.001 and *p < 0.05 as compared to the vehicle-alone control, or between specified groups, by one-way ANOVA with Tukey's multiple comparisons test.

chemokine biology and establish a novel translational foundation for the development of CXCL10-derived peptides to treat infections caused by clinically challenging bacteria.

Our current research shows that the CXCL10-derived peptide P1, which comprises the first 14 N-terminal amino acids of the mature chemokine, kills an array of bacteria under a range of conditions, including in physiologic media with and without serum. The discovery of a robust antimicrobial domain within the unstructured N-terminal region of CXCL10 expands the traditional paradigm of chemokine-mediated bactericidal

https://doi.org/10.1021/acsinfecdis.2c00456
ACS Infect. Dis. 2023, 9, 122−139

activity beyond the original focus on the C-terminal α-helix.[8] Moreover, as the N-terminus of CXCL10 is also important for binding and activating the cognate cellular receptor CXCR3,[32,34] our findings demonstrate physical overlap between determinants important for bactericidal and receptor-agonist activities. In particular, antimicrobial peptide P1 contains a three-residue amino acid motif (i.e., threonine−valine−arginine) that is fundamental to receptor recognition and signaling by CXCL10.[32,34,45] Consistent with this circumstance, peptide P1 can elicit chemotaxis by CXCR3-expressing human T-cells. These chemotactic effects, however, are markedly less than those exhibited by the full-length chemokine, presumably because peptide P1 lacks additional constituents in the N-loop region and β-sheet scaffold of CXCL10 that also contribute to high-affinity receptor binding.[32,34] Although the demonstrated overlap of host- and pathogen-targeted activities is, so far, unique to CXCL10, an analogous arrangement may be present in other chemokines. For instance, the N-terminal regions of CXCL6 and CXCL14 have also been associated, to varying degrees, with bactericidal effects.[46,47] Interestingly, the N-terminus of CXCL10, and many chemokines, is a major site of post-translational modification *in vivo* (e.g., proteolysis, citrullination, glycosylation),[48] raising the possibility that antimicrobial and receptor-based activities can be regulated or deployed independently.

The C-terminal region of CXCL10 contains a cationic α-helix with alternating stretches of hydrophilic and hydrophobic amino acid residues. Similar amphipathic structures are common among antimicrobial peptides,[21] and therefore, the C-terminus of CXCL10 has long been predicted to exert bactericidal effects.[16] The current research substantiates this capacity for the first time: P9 series peptides derived from the C-terminal region of CXCL10 were found to kill a range of bacterial species. These effects, however, were critically dependent on the presence of an ordered α-helix. In the full-length chemokine, this structural feature appears to be stabilized by extended hydrophobic contacts along the interface between the α-helix and strands of the adjacent β-sheet.[32,34] In the absence of this protein context, peptides comprising native C-terminal sequences of CXCL10 (e.g., unmodified peptide P9) were not able to assume α-helical secondary structure, or kill bacteria, under physiologic conditions. Thus, while our structure/function and alanine-scanning data highlight the importance of the linear amphipathic design of the α-helix in CXCL10-mediated antimicrobial effects, intramolecular interactions with neighboring portions of the chemokine are likely to enable and/or enhance bactericidal actions by the C-terminal region of endogenous CXCL10.

To functionalize the C-terminal antimicrobial domain of CXCL10 as a discrete and working peptide, we used hydrocarbon stapling to effectively induce and brace α-helical structure.[42] Accordingly, stapled peptide P9 exhibited durable α-helicity and significant bactericidal activity in medium with physiologic levels of salt. While not as structurally ordered as the stapled peptide, pre-stapled peptide P9, which contains non-coupled S5A residues, was also observed to adopt an α-helical conformation and kill bacteria. This finding indicates that substituting in alkene-bearing (i.e., more hydrophobic) S5A residues along the nonpolar face of the amphipathic α-helix was alone sufficient to appreciably stabilize α-helical secondary structure. Increased hydrophobicity, however, was also associated with greater cytotoxicity against human T-cells, especially by the pre-stapled peptide. The correlation between enhanced hydrophobicity and a loss of bacterial-cell selectivity has been reported for other antimicrobial peptides.[49,50] Constructively, effects against eukaryotic cells can typically be diminished or entirely eliminated (while retaining bactericidal activity) using strategies such as varying the length, position, and/or composition of the connecting staple to rebalance amphipathicity.[51,52]

By also considering prior mechanistic studies in *B. anthracis*, the current investigations reasonably identify the separate mechanisms by which the N- and C-terminus of CXCL10 exert bactericidal effects against this biodefense pathogen. Of the two known mechanisms by which CXCL10 kills *B. anthracis* bacilli, perhaps the most intriguing involves the bacterial target FtsX, the membrane-bound component of the FtsE/X mechano-transmission complex that regulates the activation of peptidoglycan hydrolases essential to bacterial growth, division, and viability.[22,23,53] In CXCL10-treated bacilli, FtsE/X becomes dysregulated, resulting in a loss of peptidoglycan integrity and subsequent cell lysis.[23] Genetic deletion of *ftsX* reduces *B. anthracis* susceptibility to CXCL10.[13,22,23] The current research found that Δ*ftsX* bacilli are also less susceptible to the antimicrobial effects of peptide P1, but not stapled peptide P9, suggesting that the N-terminal antimicrobial domain of CXCL10 mediates FtsX-dependent bactericidal activity against *B. anthracis*. Interestingly, CXCL10 has been proposed to interact directly with FtsX owing to homology between this bacterial protein and CXCR3,[13,22] the cellular receptor of CXCL10. The capacity of peptide P1 to kill bacteria and elicit chemotaxis by host immune cells is suited to this possibility. The second known mechanism of CXCL10-mediated antimicrobial activity is a comparatively non-specific disruption of membrane barrier function that collapses transmembrane potential and causes bacterial-cell death.[22,23] As discussed throughout this work and others,[8,16,21,54] the amphipathic α-helical character of the C-terminal region of CXCL10 is highly aligned with this membrane-targeted mode-of-action.

The human and economic burdens of antibiotic-resistant bacteria are significant and growing.[17,55] Toward combating these pathogens, the demonstrated capacity of CXCL10-derived peptides to kill difficult-to-treat MDR and XDR bacteria is therapeutically attractive. The N-terminal peptide P1 exerts broad-spectrum antimicrobial activity without causing hemolytic or cytotoxic effects under the conditions tested in this work. These qualities are a good starting point for antimicrobial-drug development; however, the translational prospects of peptide P1 will first depend on the ability to dissociate its dual host- and pathogen-targeted activities. Indeed, at bactericidal levels, peptide P1 elicits a phenotypic response from CXCR3-expressing immune cells. Potentially then, the administration of peptide P1 may disrupt cellular trafficking and/or provoke inflammatory damage *in vivo*.[56,57] Straightforward modifications like changing the length and/or amino acid composition of peptide P1 may be sufficient to preclude receptor-dependent actions, while also providing an opportunity to enhance bacterial killing. Regarding the C-terminus of CXCL10, functionalizing an α-helical antimicrobial domain as a stand-alone peptide is frequently limited by poor structural/functional resilience in physiologic environments. In response, stapling strategies that stabilize peptide structure and enable activity, like the approach used here to engineer the

https://doi.org/10.1021/acsinfecdis.2c00456
ACS Infect. Dis. 2023, 9, 122−139

widely functional stapled peptide P9, provide effective avenues to generate peptides with durable α-helicity and a corresponding increase in therapeutic utility.[42,52] The further development of stapled peptide P9 will benefit from improved host-cell cytocompatibility, possibly achieved by using previously successful approaches that modify the connecting staple or conjugate the peptide to another biomolecule such as a polymer.[51,58] Ultimately, future studies that include specifically tailored lead-optimization programs will be needed to effectively assess the therapeutic utility of antimicrobial CXCL10-derived peptides for treating infections caused by antibiotic-resistant bacteria.

CONCLUSION

The chemokine CXCL10 functions in host defense against infection by guiding immune cell traffic and killing microorganisms. The antimicrobial determinants of CXCL10, and how they relate to those important for cellular effects, have not been previously defined. Here, we report the discovery of disparate bactericidal domains in the N- and C-terminal regions of human CXCL10. A 14-mer peptide derived from the N-terminus of CXCL10, peptide P1, killed a broad spectrum of Gram-positive and Gram-negative bacteria, including *B. anthracis* spores and many organisms with extensive drug-resistant phenotypes such as clinical isolates of carbapenem-resistant *A. baumannii* and *K. pneumoniae*. Peptide P1 coincides with a major determinant of immune cell migration and exhibited modest chemotactic activity. A 22-mer peptide that comprised the C-terminal α-helix of CXCL10, peptide P9, was also found to be bactericidal, but only under conditions in which the peptide could form α-helical secondary structure. To overcome this limitation, we engineered a variant peptide using hydrocarbon stapling to promote α-helicity and improve functional resilience. Stapled peptide P9 exerted antimicrobial effects against a wide range of bacterial species in physiologic media. Our findings provide unique insight into the determinants of chemokine function. Moreover, that the bactericidal domains of CXCL10 can be functionalized as stand-alone peptides creates a foundation for the development of novel therapeutics to treat infections caused by antibiotic-resistant bacteria.

METHODS

Bacteria and Culture Conditions. The bacterial strains and clinical isolates used in this study are presented in Table 1. Bacteria were cultured in brain-heart infusion (BHI) broth (*B. anthracis*, *B. subtilis*, and *E. faecium*), GCBL medium containing Kellogg's supplements (*N. gonorrhoeae*),[28] or lysogeny broth (LB) Lennox (all other organisms examined herein). For preparing logarithmic-phase bacterial inoculums, organisms were grown overnight, and then sub-cultured, at 37 °C with continuous shaking (250 rpm) in tubes with loose-fitting caps; exceptions were *E. faecium* (150−200 rpm with sealed cap) and *N. gonorrhoeae* (end-over-end rotation with sealed cap). *K. pneumoniae* strains derived from ATCC 13883 and harboring an empty or *mcr-1*-encoding pBCSK construct, were grown overnight and sub-cultured in the presence of 50 μg/mL chloramphenicol. *E. coli* strain J53 (*mcr-1*+) was grown overnight in the presence of 1 μg/mL freshly prepared colistin. *B. anthracis* Sterne 7702 spores were prepared in Difco Sporulation Medium and purified by density gradient centrifugation over Percoll.[14] In this report, "multidrug-resistant" bacteria are defined as those with acquired resistance against at least one approved and useful agent in 3 or more antimicrobial categories; "extensively drug-resistant" bacteria are defined as resistant to at least one agent in all but 2 or fewer categories.[59] All bacteriologic research was conducted using biosafety level-2 precautions under the approval of the Institutional Biosafety Committee at the University of Virginia.

Table 1. Bacterial Strains Used in This Study

bacterium	strain	biosample no.	ref(s)
B. anthracis	Sterne 7702 (BA663)	SAMN07523111	15, 62
B. anthracis	Sterne 7702 Δ*ftsX*	not designated	13
B. subtilis	168 (ATCC 23857)	SAMEA3138188	63
K. pneumoniae	BL13802 (CFSAN044570)	SAMN05213500	18, 64
A. baumannii	AR0304	SAMN04901694	65
P. aeruginosa	AR0231	SAMN04901621	65
S. Typhi	BL31130 (CFSAN059647)	SAMN10086808	this work[a]
S. flexneri	BL28504 (CFSAN059650)	SAMN10086692	66
E. cloacae	BL36213 (CFSAN059636)	SAMN10086738	this work
E. faecium	AR0575	SAMN11954007	65
S. aureus	LAC (USA300)	SAMN08391108	67
N. gonorrhoeae	FA1090	SAMN02604088	28, 68
N. gonorrhoeae	H041 (WHO X)	SAMEA2448468	69, 70
K. pneumoniae	MS84 (CFSAN044565)	SAMN05213496	18, 64
K. pneumoniae	BA2664 (CFSAN044571)	SAMN05213501	18, 64
K. pneumoniae	ATCC 13883 pBCSK	not designated	18, 71
K. pneumoniae	ATCC 13883 pBCSK:: *mcr-1*	not designated	18, 71
E. coli	FI-4531	not designated	18, 72
E. coli	J53	SAMN08874679	73
E. coli	J53 *mcr-1*	not designated	18

[a]The results of antimicrobial susceptibility testing for bacterial strains not previously reported are presented in Figure S9.

Peptides. CXCL10-derived peptides, as well as sequence-scrambled and substitution variants, were synthesized by GenScript Biotech Corporation (Piscataway, New Jersey, USA) using solid-phase peptide synthesis. Peptides were amidated at their C-terminus and purified (>95%) using reverse-phase HPLC. Peptide mass was confirmed by electrospray ionization mass spectrometry. The cytolytic peptide melittin was obtained from MilliporeSigma (Burlington, Massachusetts, USA). All peptides were received as lyophilized samples and stored at −20 °C. Prior to use, peptides were reconstituted in sterile dH_2O, aliquoted into low-retention microtubes, and stored at −80 °C.

Pre-stapled and stapled peptide P9 were synthesized in-house using a CEM Corporation (Matthews, North Carolina, USA) Liberty Blue automated, microwave-assisted solid-phase peptide synthesizer via Fmoc methods on Rink amide resin (0.3 mmol/g substitution). Unless otherwise noted, reagent purities were ≥99%. Fmoc deprotection was performed using 20% (v/v) piperidine in dimethylformamide (DMF). Coupling reactions were performed using Fmoc-protected amino acids (0.2 M in DMF) obtained from Advanced Chemtech (Louisville, Kentucky, USA), and the coupling agents diisopropyl carbodiimide (1 M in DMF) and Oxyma Pure (1 M in DMF), at 90 °C for 4 min. To prevent detrimental interactions between the N-terminal amine and the metathesis

https://doi.org/10.1021/acsinfecdis.2c00456
ACS Infect. Dis. 2023, 9, 122−139

catalyst, acetyl capping of the N-terminus was achieved by reaction with acetic anhydride (≥98% pure; 1 mM in DMF), in the presence of *N,N*-diisopropylethylamine (0.1 mM in DMF) from MilliporeSigma.

To facilitate stapling, both the asparagine residue at position 8 and the alanine residue at position 12 of peptide P9 were replaced with the unnatural amino acid Fmoc-(S)-2-(4-pentenyl)-Ala-OH (≥97% pure), yielding the peptide PESKAIK(S5A)LLK(S5A)VSKERSKRSP. Stapling was then achieved on-resin through a ring-closing metathesis reaction between the S5A residues according to an application note from CEM Corporation.[60] Briefly, a 10 mM solution of Grubbs' first-generation catalyst (≥97% pure), obtained from MilliporeSigma, was prepared in dichloroethane (DCE) and deoxygenated for 20 min at room temperature with bubbled nitrogen gas. Peptide-functionalized resin was washed with DCE to remove DMF, then combined with 5 mL of the prepared catalyst solution. This mixture was reacted for 30 min at 40 °C, washed with DCE, and then reacted a second time under the same conditions. Pre-stapled peptide P9 was not subjected to the ring-closing metathesis reaction. Peptides were cleaved from the resin during a 3 h, room-temperature incubation in a cleavage cocktail consisting of 92.5% (v/v) trifluoroacetic acid (TFA), 2.5% triisopropylsilane (98% pure), 2.5% 2,2′-(ethylenedioxy)diethanethiol (95% pure), and 2.5% distilled water.

Pre-stapled and stapled peptide P9 were isolated by precipitation in cold diethyl ether and centrifugation (4800*g* for 5 min at 4 °C). After the removal of ether under vacuum, and resuspension in 95% dH_2O, 5% acetonitrile (each containing 0.1% TFA), peptides were purified by preparative-scale reverse-phase HPLC using a Waters (Milford, Massachusetts, USA) Empower chromatography system and XBridge Prep C18 5 μm optimum bed density chromatographic separation column. Peptides were eluted using an AB linear gradient of 1.6% acetonitrile per min from 5 to 40%, followed by an AB linear gradient of 0.2% acetonitrile per min from 40 to 45%, where eluent A was 0.1% aqueous TFA and eluent B was 0.1% TFA in acetonitrile. Purified peptides were lyophilized and stored at −20 °C. Purity (>95%) was confirmed by analytical reverse-phase HPLC using a Waters e2695 Alliance Separations Module and XBridge C18 3.5 μm chromatographic separation column. Analytical HPLC was performed using an AB linear gradient of 6.2% acetonitrile per min from 5 to 95%; eluent A and B were as indicated above. Peptide mass was verified using MALDI-TOF mass spectrometry performed by the University of Virginia Biomolecular Analysis Research Core with a Bruker Microflex spectrometer.

Bacterial Killing. To measure the antimicrobial effects of CXCL10-derived peptides against *B. anthracis* and *B. subtilis* bacilli, logarithmic-phase bacteria (OD_{600} ≈ 0.6) were diluted in DMEM containing 10% FBS and combined 1:1 with medium alone or containing peptides/controls in the wells of a tissue-culture treated plate (100 μL total volume; ∼2.5×10^5 cfu/mL). A reagent blank without bacteria was assayed in parallel. Following incubation (4 h at 37 °C, 5% CO_2), 10 μL of the viability reagent alamarBlue, obtained from ThermoFisher Scientific (Waltham, Massachusetts, USA), was added to each well. The sample plate was protected from light using aluminum foil and incubated until buffer-only controls demonstrated a distinct change of color from blue to pink (∼30 min). Endpoint fluorescence (excitation 530/30 nm; emission 580/20 nm) was measured using a VICTOR Nivo multi-mode plate reader by PerkinElmer (Waltham, Massachusetts, USA). Bactericidal activity against *N. gonorrhoeae* was similarly assessed, except that logarithmic-phase gonococci were exposed to peptides/controls in 0.2× of supplemented GCBL medium for 3 h at 37 °C, 5% CO_2 before the addition of alamarBlue; endpoint fluorescence was measured after overnight incubation (∼16 h) under the same conditions.

The killing of other MDR Gram-negative bacteria (*K. pneumoniae*, *A. baumannii*, *P. aeruginosa*, *S. enterica* serovar Typhi, *S. flexneri*, *E. cloacae*) and Gram-positive bacteria (*E. faecium*, *S. aureus*) following peptide exposure was measured by cfu determination and/or alamarBlue analysis. For cfu-based evaluations, logarithmic-phase bacteria (OD_{600} ≈ 0.6) were diluted to 2.5×10^5–4.0×10^5 cfu/mL in 10 mM Kph buffer (pH 7.4) + 1% TSB (v/v). Bacterial suspensions (195 μL) were combined with medium ± peptides/controls, in the wells of a tissue-culture treated plate. After incubation (2 h at 37 °C with shaking), samples were mixed by pipet and used to prepare serial dilutions in normal saline (0.9% NaCl, w/v), which were plated onto LB agar in duplicate. Colonies were enumerated following overnight growth at 37 °C.

For alamarBlue-based assessments, 2.5×10^5–4.0×10^5 cfu/mL of logarithmic-phase bacteria in RPMI 1640 medium with 2 mM L-glutamine and 25 mM HEPES buffer, or bacteria in Kph buffer + 1% TSB, were treated as described above. Reagent blanks without bacteria were included in each assay. After incubation (2 h at 37 °C with shaking), 50 μL of each sample was combined 1:1, in triplicate, with 2× LB (Lennox) medium in the wells of a fresh tissue-culture treated plate. Ten microliters of alamarBlue was added to each well, and the plate was incubated (37 °C, protected from light) until buffer-only controls demonstrated a distinct change of color (1–3 h depending on the bacterial species). Endpoint fluorescence was measured using a VICTOR Nivo multi-mode plate reader. Bacterial survival was calculated as a percentage of the species-matched untreated control according to cfu totals or blank-corrected relative fluorescence units.

Spore Germination and Viability. Prior to evaluating the potential anti-spore effects of CXCL10-derived peptides, *B. anthracis* spores (∼2×10^7 cfu/mL in sterile dH_2O) were incubated in a sterile Corning (Corning, New York, USA) Axygen Maxymum Recovery microtube for 30 min in a 70 °C water bath; this step increases spore responsiveness to nutrient germinants and eliminates any organisms that have lost dormancy. After heating, the spore suspension was briefly cooled at room temperature and then diluted to 1.5×10^5–4.0×10^5 cfu/mL in RPMI medium with 5% FBS ± individual peptides. The specific inoculum was determined by cfu determination performed in parallel by serial dilution in dH_2O and plating on BHI agar plates. Aliquots (200 μL total) of each experimental/control group were placed in duplicate into the wells of a tissue-culture treated plate. Spore germination and the outgrowth of vegetative bacilli in all samples were assessed after incubation (6 h at 37 °C, 5% CO_2) using cfu determination ± heat treatment (65 °C for 30 min before plating) to distinguish between ungerminated, viable spores (heat resistant) or germinating spores and bacilli (heat susceptible). At t = 0 and 6 h, matching sample sets in separate 96-well plates were settled by brief centrifugation (200*g* for 1 min at room temperature) and visualized using an Olympus (Waltham, Massachusetts, USA) IX71 inverted microscope equipped with a 20× relief-contrast objective and DP28 digital camera. Camera control, image capture, and scaling were

https://doi.org/10.1021/acsinfecdis.2c00456
ACS Infect. Dis. 2023, 9, 122–139

performed with cellSens v3 software (Olympus); the contrast and sharpness of photomicrographs were improved equally across all images using Adobe (San Jose, California, USA) Photoshop Elements software. At least 4 randomly chosen fields from each sample well per experiment were photographed. All results were authenticated using a second spore preparation.

RBC Hemolysis. Human subjects research was approved by the University of Virginia Institutional Review Board for Health Sciences Research (IRB-HSR; protocols #13909 and #18904). Human whole blood was collected by venipuncture and separated by density gradient centrifugation over Ficoll-Paque. Five milliliters of the RBC layer was combined with 45 mL of PBS (pH 7.4) in a 50 mL conical tube; the sample was mixed by inversion and spun at 500*g* for 10 min at room temperature. RBCs were washed twice more as above, then diluted 1:20 (v/v, 5% final) in RPMI 1640 medium with 2 mM L-glutamine and 25 mM HEPES buffer, but without phenol red, and supplemented with low-endotoxin BSA (v/v, 1% final) obtained from MilliporeSigma. Washed RBCs (180 μL) were combined in triplicate with peptides/controls (20 μL) in the wells of a round-bottom, tissue-culture treated plate. After incubation (1 h at 37 °C, 5% CO_2), the plate was spun at 500*g* for 5 min and sample supernatants (100 μL) were transferred to a clear-bottom, black-wall microplate. Absorbance (540/10 nm) was measured using a VICTOR Nivo multi-mode plate reader and normalized according to min-max scaling using RBCs exposed to buffer alone (analytical blank) or 1% Triton X-100 (complete hemolysis) to calculate percent hemolysis.

T-Cell Culture, Viability, and Chemotaxis. Peripheral blood mononuclear cells (PBMCs) were obtained from Ficoll−Paque separations of human whole blood (described above for RBC Hemolysis), and washed once each in room temperature PBS (pH 7.4) and c-RPMI (RPMI medium containing 25 mM HEPES buffer, 10% FBS, 2% penicillin-streptomycin, and 1% L-glutamine); centrifugation was performed at 500*g* for 7 min at room temperature. Washed PBMCs were suspended at 1×10^6 cells/mL in c-RPMI containing 100 IU/mL interleukin (IL)-2. CD3/CD28 Dynabeads were added to the culture (3:1, beads to cells) to activate/expand the T-cell population and induce the expression of CXCR3. After incubation (48 h at 37 °C, 5% CO_2), Dynabeads were removed from the culture using a magnetic separator. Four days post-stimulation, and every 2−3 days thereafter up to day 14, cell counts were performed and the culture density was returned to 1×10^6 cells/mL in c-RPMI containing fresh IL-2. The surface-expression of human CXCR3 was measured by flow cytometry using an Agilent (Santa Clara, California, USA) NovoCyte flow cytometer system. Receptor staining was performed with the PE-conjugated mouse IgG_1 antibodies FAB160P (anti-CXCR3) and IC002P (isotype control) from Bio-Techne (Minneapolis, Minnesota, USA).

For viability determinations, human T-cells were washed twice in RPMI medium with 25 mM HEPES buffer and 2 mM L-glutamine, and supplemented with 1% BSA, or X-VIVO 15 medium from Lonza (Morristown, New Jersey, USA). Centrifugation was performed at 400*g* for 10 min at room temperature. Cells were suspended in the same medium at 2×10^6 cells/mL and 95 μL of cells was combined in duplicate with 5 μL of peptides/controls in the wells of a flat-bottom, tissue-culture treated plate. After incubation (2 h at 37 °C, 5% CO_2), treatment samples were mixed by pipet and used for LIVE/DEAD staining with acridine orange (excitation 500 nm; emission 526 nm) + propidium iodide (excitation 533 nm; emission 617 nm) cell-viability dye from Logos Biosystems (Annandale, Virginia, USA). Cell counting, LIVE/DEAD image analysis, and viability calculations were performed using a LUNA-FL automated cell-counter with disposable PhotonSlides.

The migration of CXCR3-expressing human T-cells (cultured between 7 and 14 days post-stimulation and washed of IL-2 the day prior to analysis) was measured using the ChemoTx system by Neuro Probe (Gaithersburg, Maryland, USA). T cells (1×10^5 total per 5.7 mm site, washed and suspended in RPMI medium + 1% BSA) were loaded onto polycarbonate track-etch filters with 5 μm pores that overlaid microplate wells containing peptides/controls (300 μL total, prepared in RPMI medium + 1% BSA). Following incubation (2 h at 37 °C, 5% CO_2), non-migrated cells remaining atop the filter were removed using a multi-channel pipet and filter wiper. ChemoTx assemblies were then chilled at 4 °C for 10 min and taken apart. Cells that migrated into the lower wells were counted by flow cytometry using an Agilent NovoCyte flow cytometer system with an autosampler. Cell numbers were used to calculate chemotactic index = migrated cells in treatment group/migrated cells in buffer-only control group. Recombinant human CXCL10 was obtained from PeproTech (Cranbury, New Jersey, USA); reconstituted stocks were prepared at 0.5 mg/mL in 0.3% human serum albumin according to the manufacturer's instructions.

CD Spectroscopy. Spectra were measured under nitrogen in a 0.1 cm path length quartz-cell using a JASCO (Easton, Maryland, USA) J-1500 CD spectrophotometer with a Peltier thermostatted single-position cell holder. Unless noted otherwise, spectral accumulations (3 reads per scan) were obtained from 180 to 250 nm with a scanning speed of 50 nm/min and integration time of 1 s. Spectra Manager II software by JASCO was used to calculate mean residue ellipticity = ellipticity (mdeg)/[10 × path length (cm) × peptide concentration (M) × number of amino acid residues].

CD spectra were measured for CXCL10-derived peptides P1 and P9 (20 μM; ∼0.03−0.05 mg/mL), at 25 °C in 10 mM Kph buffer (pH 7.4), following pre-incubation (1 h at 37 °C) with buffer-alone, 50% TFE (v/v), or 800 μM of liposomes prepared using *E. coli* ATCC 11303 polar lipid extract (approximately 70% phosphatidylethanolamine, 20% phosphatidylglycerol, and 10% cardiolipin) obtained from Avanti Polar Lipids (Alabaster, Alabama, USA). Liposomes (i.e., large unilamellar vesicles) were generated by evaporating the solvent from chloroform−methanol extracted lipids, rehydrating the dried lipid film in Kph buffer (pH 7.4), freeze−thawing, and extruding through a polycarbonate membrane with 200 nm pores as previously described.[61] Spectra were also obtained for peptide P9 ± 50% TFE and the pre-stapled/stapled peptide P9 variants (40 μM; ∼0.1 mg/mL), at 25 °C in 10 mM PBS, pH 7.4. The stability of pre-stapled/stapled peptide P9 α-helicity was examined by monitoring changes in ellipticity at 222 nm as the temperature was increased from 25 to 95 °C (at 5 °C/min). Full-spectrum scans were performed at 25 °C both before and after heating. Secondary structure determination and fold recognition prediction from CD spectra were performed using the BeStSel (Beta Structure Selection) Web server available at https://bestsel.elte.hu/index.php.[36]

https://doi.org/10.1021/acsinfecdis.2c00456
ACS Infect. Dis. 2023, 9, 122−139

Statistics and Graphing. All experimental analyses were conducted in replicate and independently repeated. Statistical evaluations, curve fitting, and graphing were performed using GraphPad Prism 9 software. Statistically significant differences among treatment groups were determined using one-way analysis of variance (ANOVA) with Dunnett's or Tukey's multiple comparisons test; a p value <0.05 was considered to be significant. The EC_{50} values of CXCL10-derived bactericidal peptides were determined by nonlinear regression using sigmoidal dose−response (variable slope) or bell-shaped equations, as appropriate, and are reported ±95% confidence interval.

■ ASSOCIATED CONTENT

Supporting Information

The Supporting Information is available free of charge at https://pubs.acs.org/doi/10.1021/acsinfecdis.2c00456.

Figures S1−S9 (PDF)

■ AUTHOR INFORMATION

Corresponding Author

Molly A. Hughes − *Division of Infectious Diseases and International Health, Department of Medicine, University of Virginia, Charlottesville, Virginia 22908, United States;* Phone: 1 (434) 924-2600; Email: mah3x@virginia.edu

Authors

Matthew A. Crawford − *Division of Infectious Diseases and International Health, Department of Medicine, University of Virginia, Charlottesville, Virginia 22908, United States;* orcid.org/0000-0003-0404-0061

Amanda E. Ward − *Department of Molecular Physiology and Biological Physics, University of Virginia, Charlottesville, Virginia 22908, United States;* orcid.org/0000-0001-8184-0447

Vincent Gray − *Department of Chemical Engineering, University of Virginia, Charlottesville, Virginia 22904, United States*

Peter Bailer − *Department of Molecular Physiology and Biological Physics, University of Virginia, Charlottesville, Virginia 22908, United States;* Present Address: Perelman School of Medicine, University of Pennsylvania, Philadelphia, Pennsylvania 19104, USA; orcid.org/0000-0002-3865-6932

Debra J. Fisher − *Division of Infectious Diseases and International Health, Department of Medicine, University of Virginia, Charlottesville, Virginia 22908, United States*

Ewa Kubicka − *Division of Hematology and Oncology, Department of Medicine, University of Virginia, Charlottesville, Virginia 22908, United States;* Present Address: Office of Research Core Administration, University of Virginia, Charlottesville, Virginia 22903, USA

Zixian Cui − *Department of Chemical Engineering, University of Virginia, Charlottesville, Virginia 22904, United States*

Qinmo Luo − *Department of Chemical Engineering, University of Virginia, Charlottesville, Virginia 22904, United States;* Present Address: Merck & Company Inc., Elkton, Virginia 22827, USA

Mary C. Gray − *Department of Microbiology, Immunology, and Cancer Biology, University of Virginia, Charlottesville, Virginia 22908, United States*

Alison K. Criss − *Department of Microbiology, Immunology, and Cancer Biology, University of Virginia, Charlottesville, Virginia 22908, United States*

Lawrence G. Lum − *Division of Hematology and Oncology, Department of Medicine, University of Virginia, Charlottesville, Virginia 22908, United States*

Lukas K. Tamm − *Department of Molecular Physiology and Biological Physics, University of Virginia, Charlottesville, Virginia 22908, United States;* orcid.org/0000-0002-1674-4464

Rachel A. Letteri − *Department of Chemical Engineering, University of Virginia, Charlottesville, Virginia 22904, United States*

Complete contact information is available at: https://pubs.acs.org/10.1021/acsinfecdis.2c00456

Author Contributions

M.A.C., A.E.W., E.K., M.C.G., L.G.L., R.A.L., and M.A.H. conceived and designed experiments; V.G., Z.C., and Q.L. synthesized and purified peptides; M.A.C., A.E.W., V.G., D.J.F., P.B., E.K., Z.C., Q.L., and M.C.G. performed experiments; M.A.C., A.E.W., V.G., D.J.F., P.B., E.K., R.A.L., and M.A.H. analyzed data; M.A.C., V.G., and E.K. prepared figures; A.K.C., L.G.L., L.K.T., R.A.L., and M.A.H. contributed bacterial isolates, human-derived materials, and/or other unique resources; M.A.C., A.E.W., V.G., R.A.L., and M.A.H. wrote the manuscript. All authors reviewed study results and approved this report.

Notes

The authors declare no competing financial interest.

■ ACKNOWLEDGMENTS

The authors thank Katie R. Margulieux and Arpita Singh (University of Virginia) for assistance with preliminary studies, Nixon M. Crawford (Charlottesville, VA) for generating scrambled peptide sequences, Erum Khan (Aga Khan University) for providing clinical isolates, and Christine Lascols (CDC) for performing antimicrobial susceptibility testing. This research was supported by The Ivy Foundation and Global Infectious Diseases Institute at the University of Virginia, and by the National Institute of Allergy and Infectious Diseases Grant R01 AI150941. Additional support for this work was received from the National Institutes of Health Fellowship F30 HD101348 and Training Grants T32 GM007267 and T32 GM080186 (A.E.W.), as well as Grants R01 AI30557 (L.K.T.) and R01 AI097312 (M.C.G. and A.K.C.). The Table of Contents graphic was created with BioRender.com.

■ ABBREVIATIONS

ANOVA, analysis of variance; BeStSel, Beta Structure Selection; BHI, brain−heart infusion; BSA, bovine serum albumin; CD, circular dichroism; CDC, U.S. Centers for Disease Control and Prevention; cfu, colony-forming unit; CI, chemotactic index; CXCL, C-X-C motif chemokine ligand; CXCR, C-X-C motif chemokine receptor; DCE, dichloroethane; DMEM, Dulbecco's Modified Eagle Medium; DMF, dimethylformamide; EC_{50}, half-maximal effective concentration; *Ec*, *Escherichia coli*; ESBL, extended-spectrum beta-lactamase; EtOH, ethanol; FBS, fetal bovine serum; *fts*, filamentation temperature-sensitive; GCBL, gonococcal base liquid; HPLC, high-performance liquid chromatography; HSR,

Health Sciences Research; IL, interleukin; IP-10, interferon γ-induced protein 10 kDa; IRB, institutional review board; *Kp*, *Klebsiella pneumoniae*; Kph, potassium phosphate buffer; L-Ara4N, 4-amino-4-deoxy-L-arabinose; LB, lysogeny broth; LPS, lipopolysaccharide; MALDI, matrix-assisted laser desorption/ionization; MBL, metallo-beta-lactamase; *mcr*, mobilized colistin resistance; MDR, multidrug-resistant; MIC, minimum inhibitory concentration; MRSA, methicillin-resistant *Staphylococcus aureus*; nd, none detected; NDM, New Delhi metallo-beta-lactamase; *Ng*, *Neisseria gonorrheae*; ns, not significant; nt, not tested; OXA, oxacillinase; PBMC, peripheral blood mononuclear cells; PBS, phosphate-buffered saline; PE, phycoerythrin; pEtN, phosphoethanolamine; PL, polar lipids; POS, positive; RBC, red blood cell; RFU, relative fluorescence unit; RPMI, Roswell Park Memorial Institute; S5A, (*S*)-2-(4-pentenyl)-Ala-OH; SD, standard deviation; TFA, trifluoroacetic acid; TFE, 2,2,2-trifluoroethanol; TOF, time-of-flight; TSB, tryptic soy broth; VRE, vancomycin-resistant *Enterococcus*; wt, wild-type; XDR, extensively drug-resistant

REFERENCES

(1) Griffith, J. W.; Sokol, C. L.; Luster, A. D. Chemokines and chemokine receptors: positioning cells for host defense and immunity. *Annu. Rev. Immunol.* **2014**, *32*, 659−702.

(2) Söbirk, S. K.; Mörgelin, M.; Egesten, A.; Bates, P.; Shannon, O.; Collin, M. Human chemokines as antimicrobial peptides with direct parasiticidal effect on *Leishmania mexicana in vitro*. *PloS One* **2013**, *8* (3), e58129.

(3) Nakayama, T.; Shirane, J.; Hieshima, K.; Shibano, M.; Watanabe, M.; Jin, Z.; Nagakubo, D.; Saito, T.; Shimomura, Y.; Yoshie, O. Novel antiviral activity of chemokines. *Virology* **2006**, *350* (2), 484−492.

(4) Hieshima, K.; Ohtani, H.; Shibano, M.; Izawa, D.; Nakayama, T.; Kawasaki, Y.; Shiba, F.; Shiota, M.; Katou, F.; Saito, T.; Yoshie, O. CCL28 has dual roles in mucosal immunity as a chemokine with broad-spectrum antimicrobial activity. *J. Immunol.* **2003**, *170* (3), 1452−1461.

(5) Yang, D.; Chen, Q.; Hoover, D. M.; Staley, P.; Tucker, K. D.; Lubkowski, J.; Oppenheim, J. J. Many chemokines including CCL20/MIP-3alpha display antimicrobial activity. *J. Leukoc Biol.* **2003**, *74* (3), 448−455.

(6) Miller, M. C.; Mayo, K. H. Chemokines from a structural perspective. *Int. J. Mol. Sci.* **2017**, *18* (10), E2088.

(7) Fernandez, E. J.; Lolis, E. Structure, function, and inhibition of chemokines. *Annu. Rev. Pharmacol. Toxicol.* **2002**, *42*, 469−499.

(8) Crawford, M. A.; Margulieux, K. R.; Singh, A.; Nakamoto, R. K.; Hughes, M. A. Mechanistic insights and therapeutic opportunities of antimicrobial chemokines. *Semin. Cell Dev. Biol.* **2019**, *88*, 119−128.

(9) Arimont, M.; Sun, S. L.; Leurs, R.; Smit, M.; de Esch, I. J. P.; de Graaf, C. Structural analysis of chemokine receptor-ligand interactions. *J. Med. Chem.* **2017**, *60* (12), 4735−4779.

(10) Metzemaekers, M.; Vanheule, V.; Janssens, R.; Struyf, S.; Proost, P. Overview of the mechanisms that may contribute to the non-redundant activities of interferon-inducible CXC chemokine receptor 3 ligands. *Front Immunol.* **2018**, *8*, 1970.

(11) Schutte, K. M.; Fisher, D. J.; Burdick, M. D.; Mehrad, B.; Mathers, A. J.; Mann, B. J.; Nakamoto, R. K.; Hughes, M. A. *Escherichia coli* pyruvate dehydrogenase complex is an important component of CXCL10-mediated antimicrobial activity. *Infect. Immun.* **2016**, *84* (1), 320−328.

(12) Holdren, G. O.; Rosenthal, D. J.; Yang, J.; Bates, A. M.; Fischer, C. L.; Zhang, Y.; Brogden, N. K.; Brogden, K. A. Antimicrobial activity of chemokine CXCL10 for dermal and oral microorganisms. *Antibiotics (Basel)* **2014**, *3* (4), 527−539.

(13) Crawford, M. A.; Lowe, D. E.; Fisher, D. J.; Stibitz, S.; Plaut, R. D.; Beaber, J. W.; Zemansky, J.; Mehrad, B.; Glomski, I. J.; Strieter, R. M.; Hughes, M. A. Identification of the bacterial protein FtsX as a unique target of chemokine-mediated antimicrobial activity against *Bacillus anthracis*. *Proc. Natl. Acad. Sci. U. S. A.* **2011**, *108* (41), 17159−17164.

(14) Crawford, M. A.; Burdick, M. D.; Glomski, I. J.; Boyer, A. E.; Barr, J. R.; Mehrad, B.; Strieter, R. M.; Hughes, M. A. Interferon-inducible CXC chemokines directly contribute to host defense against inhalational anthrax in a murine model of infection. *PLoS Pathog.* **2010**, *6* (11), e1001199.

(15) Crawford, M. A.; Zhu, Y.; Green, C. S.; Burdick, M. D.; Sanz, P.; Alem, F.; O'Brien, A. D.; Mehrad, B.; Strieter, R. M.; Hughes, M. A. Antimicrobial effects of interferon-inducible CXC chemokines against *Bacillus anthracis* spores and bacilli. *Infect. Immun.* **2009**, *77* (4), 1664−1678.

(16) Cole, A. M.; Ganz, T.; Liese, A. M.; Burdick, M. D.; Liu, L.; Strieter, R. M. Cutting edge: IFN-inducible ELR$^-$ CXC chemokines display defensin-like antimicrobial activity. *J. Immunol.* **2001**, *167* (2), 623−627.

(17) Centers for Disease Control and Prevention. Antibiotic resistance threats in the United States, 2019 U.S. Department of Health and Human Services, 2019; https://www.cdc.gov/drugresistance/biggest-threats.html.

(18) Crawford, M. A.; Fisher, D. J.; Leung, L. M.; Lomonaco, S.; Lascols, C.; Cannatelli, A.; Giani, T.; Rossolini, G. M.; Doi, Y.; Goodlett, D. R.; Allard, M. W.; Sharma, S. K.; Khan, E.; Ernst, R. K.; Hughes, M. A. CXC chemokines exhibit bactericidal activity against multidrug-resistant Gram-negative pathogens. *mBio* **2017**, *8* (6), e01549-17.

(19) Egesten, A.; Eliasson, M.; Johansson, H. M.; Olin, A. I.; Morgelin, M.; Mueller, A.; Pease, J. E.; Frick, I. M.; Bjorck, L. The CXC chemokine MIG/CXCL9 is important in innate immunity against *Streptococcus pyogenes*. *J. Infect. Dis.* **2007**, *195* (5), 684−693.

(20) Reid-Yu, S. A.; Tuinema, B. R.; Small, C. N.; Xing, L.; Coombes, B. K. CXCL9 contributes to antimicrobial protection of the gut during *Citrobacter rodentium* infection independent of chemokine-receptor signaling. *PLoS Pathog.* **2015**, *11* (2), e1004648.

(21) Jenssen, H.; Hamill, P.; Hancock, R. E. W. Peptide antimicrobial agents. *Clin. Microbiol. Rev.* **2006**, *19* (3), 491−511.

(22) Margulieux, K. R.; Fox, J. W.; Nakamoto, R. K.; Hughes, M. A. CXCL10 acts as a bifunctional antimicrobial molecule against *Bacillus anthracis*. *mBio* **2016**, *7* (3), e00334-16.

(23) Margulieux, K. R.; Liebov, B. K.; Tirumala, V. S. K. K. S.; Singh, A.; Bushweller, J. H.; Nakamoto, R. K.; Hughes, M. A. *Bacillus anthracis* peptidoglycan integrity is disrupted by the chemokine CXCL10 through the FtsE/X complex. *Front. Microbiol.* **2017**, *8*, 740.

(24) Shiloh, M. U.; Ruan, J.; Nathan, C. Evaluation of bacterial survival and phagocyte function with a fluorescence-based microplate assay. *Infect. Immun.* **1997**, *65* (8), 3193−3198.

(25) Bruce, K. E.; Rued, B. E.; Tsui, H. C. T.; Winkler, M. E. The Opp (AmiACDEF) oligopeptide transporter mediates resistance of serotype-2 *Streptococcus pneumoniae* D39 to killing by chemokine CXCL10 and other antimicrobial peptides. *J. Bacteriol.* **2018**, *200* (11), e00745−17.

(26) Huang, H. W. Molecular mechanism of antimicrobial peptides: the origin of cooperativity. *Biochim. Biophys. Acta* **2006**, *1758* (9), 1292−1302.

(27) Han, S.; Bishop, B. M.; van Hoek, M. L. Antimicrobial activity of human beta-defensins and induction by *Francisella*. *Biochem. Biophys. Res. Commun.* **2008**, *371* (4), 670−674.

(28) Ball, L. M.; Criss, A. K. Constitutively Opa-expressing and Opa-deficient *Neisseria gonorrhoeae* strains differentially stimulate and survive exposure to human neutrophils. *J. Bacteriol.* **2013**, *195* (13), 2982−2990.

(29) Binsker, U.; Käsbohrer, A.; Hammerl, J. A. Global colistin use: a review of the emergence of resistant *Enterobacterales* and the impact on their genetic basis. *FEMS Microbiol Rev.* **2022**, *46* (1), fuab049.

(30) Sabnis, A.; Hagart, K. L.; Klöckner, A.; Becce, M.; Evans, L. E.; Furniss, R. C. D.; Mavridou, D. A.; Murphy, R.; Stevens, M. M.; Davies, J. C.; Larrouy-Maumus, G. J.; Clarke, T. B.; Edwards, A. M. Colistin kills bacteria by targeting lipopolysaccharide in the cytoplasmic membrane. *eLife* **2021**, *6* (10), e65836.

https://doi.org/10.1021/acsinfecdis.2c00456
ACS Infect. Dis. 2023, 9, 122−139

(31) Napier, B. A.; Burd, E. M.; Satola, S. W.; Cagle, S. M.; Ray, S. M.; McGann, P.; Pohl, J.; Lesho, E. P.; Weiss, D. S. Clinical use of colistin induces cross-resistance to host antimicrobials in *Acinetobacter baumannii*. *mBio* **2013**, *4* (3), e00021-13.
(32) Campanella, G. S. V.; Lee, E. M. J.; Sun, J.; Luster, A. D. CXCR3 and heparin binding sites of the chemokine IP-10 (CXCL10). *J. Biol. Chem.* **2003**, *278* (19), 17066−17074.
(33) Swaminathan, G. J.; Holloway, D. E.; Colvin, R. A.; Campanella, G. K.; Papageorgiou, A. C.; Luster, A. D.; Acharya, K. R. Crystal structures of oligomeric forms of the IP-10/CXCL10 chemokine. *Structure* **2003**, *11* (5), 521−532.
(34) Booth, V.; Keizer, D. W.; Kamphuis, M. B.; Clark-Lewis, I.; Sykes, B. D. The CXCR3 binding chemokine IP-10/CXCL10: structure and receptor interactions. *Biochemistry* **2002**, *41* (33), 10418−10425.
(35) Roccatano, D.; Colombo, G.; Fioroni, M.; Mark, A. E. Mechanism by which 2,2,2-trifluoroethanol/water mixtures stabilize secondary-structure formation in peptides: a molecular dynamics study. *Proc. Natl. Acad. Sci. U. S. A.* **2002**, *99* (19), 12179−12184.
(36) Micsonai, A.; Wien, F.; Kernya, L.; Lee, Y. H.; Goto, Y.; Réfrégiers, M.; Kardos, J. Accurate secondary structure prediction and fold recognition for circular dichroism spectroscopy. *Proc. Natl. Acad. Sci. U. S. A.* **2015**, *112* (24), E3095−3103.
(37) Fernández-Vidal, M.; Jayasinghe, S.; Ladokhin, A. S.; White, S. H. Folding amphipathic helices into membranes: amphiphilicity trumps hydrophobicity. *J. Mol. Biol.* **2007**, *370* (3), 459−470.
(38) Park, I. Y.; Cho, J. H.; Kim, K. S.; Kim, Y. B.; Kim, M. S.; Kim, S. C. Helix stability confers salt resistance upon helical antimicrobial peptides. *J. Biol. Chem.* **2004**, *279* (14), 13896−13901.
(39) Travis, S. M.; Anderson, N. N.; Forsyth, W. R.; Espiritu, C.; Conway, B. D.; Greenberg, E. P.; McCray, P. B.; Lehrer, R. I.; Welsh, M. J.; Tack, B. F. Bactericidal activity of mammalian cathelicidin-derived peptides. *Infect. Immun.* **2000**, *68* (5), 2748−2755.
(40) Turner, J.; Cho, Y.; Dinh, N. N.; Waring, A. J.; Lehrer, R. I. Activities of LL-37, a cathelin-associated antimicrobial peptide of human neutrophils. *Antimicrob. Agents Chemother.* **1998**, *42* (9), 2206−2214.
(41) Smith, J. S.; Scholtz, J. M. Energetics of polar side-chain interactions in helical peptides: salt effects on ion pairs and hydrogen bonds. *Biochemistry* **1998**, *37* (1), 33−40.
(42) Walensky, L. D.; Bird, G. H. Hydrocarbon-stapled peptides: principles, practice, and progress. *J. Med. Chem.* **2014**, *57* (15), 6275−6288.
(43) Galdino, A. C. M.; Branquinha, M. H.; Santos, A. L. S.; Viganor, L. *Pseudomonas aeruginosa* and its arsenal of proteases: weapons to battle the host. In *Pathophysiological Aspects of Proteases*; Chakraborti, S., Dhalla, N. S., Eds.; Springer: Singapore, 2017; pp 381−397. DOI: 10.1007/978-981-10-6141-7_16
(44) López-Cotarelo, P.; Gómez-Moreira, C.; Criado-García, O.; Sánchez, L.; Rodríguez-Fernández, J. L. Beyond chemoattraction: Multifunctionality of chemokine receptors in leukocytes. *Trends Immunol.* **2017**, *38* (12), 927−941.
(45) Rollins, B. J. Chemokines. *Blood* **1997**, *90* (3), 909−928.
(46) Dai, C.; Basilico, P.; Cremona, T. P.; Collins, P.; Moser, B.; Benarafa, C.; Wolf, M. CXCL14 displays antimicrobial activity against respiratory tract bacteria and contributes to clearance of *Streptococcus pneumoniae* pulmonary infection. *J. Immunol.* **2015**, *194* (12), 5980−5989.
(47) Linge, H. M.; Collin, M.; Nordenfelt, P.; Mörgelin, M.; Malmsten, M.; Egesten, A. The human CXC chemokine granulocyte chemotactic protein 2 (GCP-2)/CXCL6 possesses membrane-disrupting properties and is antibacterial. *Antimicrob. Agents Chemother.* **2008**, *52* (7), 2599−2607.
(48) Vanheule, V.; Metzemaekers, M.; Janssens, R.; Struyf, S.; Proost, P. How post-translational modifications influence the biological activity of chemokines. *Cytokine* **2018**, *109*, 29−51.
(49) Frederiksen, N.; Hansen, P. R.; Björkling, F.; Franzyk, H. Peptide/peptoid hybrid oligomers: The influence of hydrophobicity and relative side-chain length on antibacterial activity and cell selectivity. *Molecules* **2019**, *24* (24), E4429.
(50) Chen, Y.; Guarnieri, M. T.; Vasil, A. I.; Vasil, M. L.; Mant, C. T.; Hodges, R. S. Role of peptide hydrophobicity in the mechanism of action of alpha-helical antimicrobial peptides. *Antimicrob. Agents Chemother.* **2007**, *51* (4), 1398−1406.
(51) Mourtada, R.; Herce, H. D.; Yin, D. J.; Moroco, J. A.; Wales, T. E.; Engen, J. R.; Walensky, L. D. Design of stapled antimicrobial peptides that are stable, nontoxic and kill antibiotic-resistant bacteria in mice. *Nat. Biotechnol.* **2019**, *37* (10), 1186−1197.
(52) Sawyer, T. K.; Partridge, A. W.; Kaan, H. Y. K.; Juang, Y. C.; Lim, S.; Johannes, C.; Yuen, T. Y.; Verma, C.; Kannan, S.; Aronica, P.; Tan, Y. S.; Sherborne, B.; Ha, S.; Hochman, J.; Chen, S.; Surdi, L.; Peier, A.; Sauvagnat, B.; Dandliker, P. J.; Brown, C. J.; Ng, S.; Ferrer, F.; Lane, D. P. Macrocyclic α-helical peptide therapeutic modality: A perspective of learnings and challenges. *Bioorg. Med. Chem.* **2018**, *26* (10), 2807−2815.
(53) Pichoff, S.; Du, S.; Lutkenhaus, J. Roles of FtsEX in cell division. *Res. Microbiol.* **2019**, *170* (8), 374−380.
(54) Kabelka, I.; Vácha, R. Advances in molecular understanding of α-helical membrane-active peptides. *Acc. Chem. Res.* **2021**, *54* (9), 2196−2204.
(55) Antimicrobial Resistance Collaborators. Global burden of bacterial antimicrobial resistance in 2019: a systematic analysis. *Lancet* **2022**, *399* (10325), 629−655.
(56) Callahan, V.; Hawks, S.; Crawford, M. A.; Lehman, C. W.; Morrison, H. A.; Ivester, H. M.; Akhrymuk, I.; Boghdeh, N.; Flor, R.; Finkielstein, C. V.; Allen, I. C.; Weger-Lucarelli, J.; Duggal, N.; Hughes, M. A.; Kehn-Hall, K. The pro-inflammatory chemokines CXCL9, CXCL10 and CXCL11 are upregulated following SARS-CoV-2 infection in an AKT-dependent manner. *Viruses* **2021**, *13* (6), 1062.
(57) Antonelli, A.; Ferrari, S. M.; Giuggioli, D.; Ferrannini, E.; Ferri, C.; Fallahi, P. Chemokine (C-X-C motif) ligand (CXCL)10 in autoimmune diseases. *Autoimmun. Rev.* **2014**, *13* (3), 272−280.
(58) Cui, Z.; Luo, Q.; Bannon, M. S.; Gray, V. P.; Bloom, T. G.; Clore, M. F.; Hughes, M. A.; Crawford, M. A.; Letteri, R. A. Molecular engineering of antimicrobial peptide (AMP)-polymer conjugates. *Biomater. Sci.* **2021**, *9* (15), 5069−5091.
(59) Magiorakos, A. P.; Srinivasan, A.; Carey, R. B.; Carmeli, Y.; Falagas, M. E.; Giske, C. G.; Harbarth, S.; Hindler, J. F.; Kahlmeter, G.; Olsson-Liljequist, B.; Paterson, D. L.; Rice, L. B.; Stelling, J.; Struelens, M. J.; Vatopoulos, A.; Weber, J. T.; Monnet, D. L. Multidrug-resistant, extensively drug-resistant and pandrug-resistant bacteria: an international expert proposal for interim standard definitions for acquired resistance. *Clin. Microbiol. Infect.* **2012**, *18* (3), 268−281.
(60) CEM Corporation. Automated synthesis of hydrocarbon-stapled peptides via microwave assisted ring-closing metathesis, Application Note ap0139, 2018; https://cem.com/en/automated-synthesis-of-hydrocarbon-stapled-peptides-via-microwave-assisted-ring-closing-metathesis.
(61) Pokorny, A.; Almeida, P. F. F. Kinetics of dye efflux and lipid flip-flop induced by delta-lysin in phosphatidylcholine vesicles and the mechanism of graded release by amphipathic, alpha-helical peptides. *Biochemistry* **2004**, *43* (27), 8846−8857.
(62) Staab, A.; Plaut, R. D.; Pratt, C.; Lovett, S. P.; Wiley, M. R.; Biggs, T. D.; Bernhards, R. C.; Beck, L. C.; Palacios, G. F.; Stibitz, S.; Jones, K. L.; Goodwin, B. G.; Smith, M. A.; Sozhamannan, S. Whole-genome sequences of variants of *Bacillus anthracis* Sterne and their toxin gene deletion mutants. *Genome Announc.* **2017**, *5* (45), e01231-17.
(63) Zeigler, D. R.; Prágai, Z.; Rodriguez, S.; Chevreux, B.; Muffler, A.; Albert, T.; Bai, R.; Wyss, M.; Perkins, J. B. The origins of 168, W23, and other *Bacillus subtilis* legacy strains. *J. Bacteriol.* **2008**, *190* (21), 6983−6995.
(64) Crawford, M. A.; Timme, R.; Lomonaco, S.; Lascols, C.; Fisher, D. J.; Sharma, S. K.; Strain, E.; Allard, M. W.; Brown, E. W.; McFarland, M. A.; Croley, T.; Hammack, T. S.; Weigel, L. M.;

Anderson, K.; Hodge, D. R.; Pillai, S. P.; Morse, S. A.; Khan, E.; Hughes, M. A. Genome sequences of multidrug-resistant, colistin-susceptible and -resistant *Klebsiella pneumoniae* clinical isolates from Pakistan. *Genome Announc.* **2016**, *4* (6), e01419-16.
(65) Lutgring, J. D.; Machado, M. J.; Benahmed, F. H.; Conville, P.; Shawar, R. M.; Patel, J.; Brown, A. C. FDA-CDC Antimicrobial Resistance Isolate Bank: a publicly available resource to support research, development, and regulatory requirements. *J. Clin Microbiol.* **2018**, *56* (2), e01415-17.
(66) Lomonaco, S.; Lascols, C.; Crawford, M. A.; Anderson, K.; Hodge, D. R.; Fisher, D. J.; Pillai, S. P.; Morse, S. A.; Khan, E.; Hughes, M. A.; Allard, M. W.; Sharma, S. K. Draft genome sequences of antimicrobial-resistant *Shigella* clinical isolates from Pakistan. *Microbiol. Resour. Announc.* **2019**, *8* (30), e00500-19.
(67) Kennedy, A. D.; Otto, M.; Braughton, K. R.; Whitney, A. R.; Chen, L.; Mathema, B.; Mediavilla, J. R.; Byrne, K. A.; Parkins, L. D.; Tenover, F. C.; Kreiswirth, B. N.; Musser, J. M.; DeLeo, F. R. Epidemic community-associated methicillin-resistant *Staphylococcus aureus*: Recent clonal expansion and diversification. *Proc. Natl. Acad. Sci. U. S. A.* **2008**, *105* (4), 1327−1332.
(68) Dempsey, J. A.; Litaker, W.; Madhure, A.; Snodgrass, T. L.; Cannon, J. G. Physical map of the chromosome of *Neisseria gonorrhoeae* FA1090 with locations of genetic markers, including opa and pil genes. *J. Bacteriol.* **1991**, *173* (17), 5476−5486.
(69) Unemo, M.; Golparian, D.; Sánchez-Busó, L.; Grad, Y.; Jacobsson, S.; Ohnishi, M.; Lahra, M. M.; Limnios, A.; Sikora, A. E.; Wi, T.; Harris, S. R. The novel 2016 WHO *Neisseria gonorrhoeae* reference strains for global quality assurance of laboratory investigations: phenotypic, genetic and reference genome characterization. *J. Antimicrob. Chemother.* **2016**, *71* (11), 3096−3108.
(70) Ohnishi, M.; Golparian, D.; Shimuta, K.; Saika, T.; Hoshina, S.; Iwasaku, K.; Nakayama, S.-i.; Kitawaki, J.; Unemo, M. Is *Neisseria gonorrhoeae* initiating a future era of untreatable gonorrhea?: Detailed characterization of the first strain with high-level resistance to ceftriaxone. *Antimicrob. Agents Chemother.* **2011**, *55* (7), 3538−3545.
(71) Liu, Y. Y.; Chandler, C. E.; Leung, L. M.; McElheny, C. L.; Mettus, R. T.; Shanks, R. M. Q.; Liu, J. H.; Goodlett, D. R.; Ernst, R. K.; Doi, Y. Structural modification of lipopolysaccharide conferred by *mcr-1* in Gram-negative ESKAPE pathogens. *Antimicrob. Agents Chemother.* **2017**, *61* (6), e00580-17.
(72) Cannatelli, A.; Giani, T.; Antonelli, A.; Principe, L.; Luzzaro, F.; Rossolini, G. M. First detection of the *mcr-1* colistin resistance gene in *Escherichia coli* in Italy. *Antimicrob. Agents Chemother.* **2016**, *60* (5), 3257−3258.
(73) Yi, H.; Cho, Y. J.; Yong, D.; Chun, J. Genome sequence of *Escherichia coli* J53, a reference strain for genetic studies. *J. Bacteriol.* **2012**, *194* (14), 3742−3743.

https://doi.org/10.1021/acsinfecdis.2c00456
ACS Infect. Dis. 2023, 9, 122−139